W-AM-Min2-1 CROSS-BRIDGE ORDER AND ORIENTATION IN RESTING AND ACTIVE MUSCLE FIBERS STUDIED BY LINEAR DICHROISM OF BOUND RHODAMINE LABEL. Julian Borejdo and Thomas P. Burghardt, CVRI, University of California, Medical Center, San Francisco, Ca. 94143.
Linear dichroism of iodoacetyl rhodamine labels attached to the single reactive thiol of the myosin heads was measured to determine the spatial orientation and the degree of order in myosin cross-bridges in single, glycerinated fibers in rest and during contraction. We have previously shown that in rigor the chromophoric labels are well ordered and that in the presence of MgADP a large fraction of probes remains ordered but assumes attitude different from rigor. Here we show that in relaxed muscle the probe order is dependent on ionic strength : at and above 120 mM there is no evident probe orientation implying a high degree of cross-bridge disorder. Below 100 mM there is progressively more order with decreasing ionic strength, peaking at 40 mM (below which no measurements could be taken at room temperature). The order observed under these conditions is rigor-like, and assuming cross-bridge angle to be identical to the rigor angle, it can be calculated to be due to the orientation of 20% of the total number of cross-bridges, the rest assuming random orientation. Stretching the muscle beyond the point of overlap between actin- and myosin-containig filaments does not affect the ionic strength dependence of the amount of order present in relaxed muscle suggesting that the observed order is due to ionic interactions of cross-bridges with the thick filament core. During isometric contraction a large fraction of the probes shows a high degree of order suggesting the attachment of 70% of the cross-bridges to actin. The ordered cross-bridges have probe attitude identical to that of the MgADP-induced state, suggesting that the transition from MgADP state to the following (most likely rigor) state is rate limiting in the mechanical cycle of the cross-bridge in isometric activity.

W-AM-Min2-2 LASER LIGHT SCATTERING STUDIES OF ACTIVE AND PASSIVE CROSS-BRIDGE MOTIONS OF MUSCLE FILAMENTS IN SUSPENSION. B. Chu, S.-F. Fan, M.M. Dewey, B. Gaylinn, D. Colflesh and R. Greguski. State Univerity of New York at Stony Brook, L.I., N.Y. 11794.

Upon the addition of Ca^{2+} to a suspension of isolated Limulus thick filaments containing ATP, quasielastic light scattering has been used successfully as a probe to detect an increase in high-frequency internal motions of the filaments. We have attributed the high-frequency characteristic times mainly to active cross-bridge motions instead of an increase in filament flexibility. Experiments have been performed to strengthen this supposition. These include suppression of the additional high-frequency motions by removal or thermal denaturation of the cross-bridges, by using vanadate to deplete the energy supply through inhibition of myosin ATPase activity, and by replacing ATP with non-hydrolyzable CrADP or AMP PNP.

If we treat the filament suspension in a relaxing solution with an anti-calmodulin agent, trifluoroperazine (TFP), no active cross-bridge motions are observed upon the addition of Ca^{2+}. Once the cross-bridge motions have been activated, TFP cannot suppress the additional high-frequency internal motions. Yet calmodulin cannot remove the suppressing effect of TFP so long as TFP is present before the addition of calcium ions. The serine protease inhibitor, phenylmethylsulfonyl fluoride (PMSF) can suppress active cross-bridge motions without affecting the Ca^{2+}-dependent myosin ATPase activity. If ATP is removed from the filament suspension by dialysis, high-frequency motions which are insensitive to heat denaturation and PMSF but sensitive to TFP has been observed in the absence and presence of Ca^{2+}. We now speculate the latter characteristic times to be those of passive thermal motions of the cross bridges.

W-AM-Min2-3 TRIPLET PROBE STUDY OF RESTRICTED MOTION IN MYOSIN MONOMERS AND FILAMENTS
Thomas M. Eads, Robert H. Bennett and David D. Thomas, Biochemistry Department, University of Minnesota Medical School, Minneapolis, MN 55455.

Rotational diffusion of myosin heads in monomer and in filaments (0.5 and 0.12 M KCl, resp., 5mM $MgCl_2$, 1 EGTA, 1 NaN_3, 25 MOPS, pH 7.0) was observed at 4°C by time-resolved absorbance anisotropy of eosin specifically and covalently bound to sulfhydryl-1 on the head. Long triplet lifetimes allowed analysis of data in the microsecond range:

	A_1	ϕ_1	A_2	ϕ_2	A_3	least squares fit of data to:
monomer	.56	.40	.35	2.6	.06	$A_1\exp(-t/\phi_1) + A_2\exp(-t/\phi_2) + A_3$;
filament	.43	.73	.31	4.9	.26	$A_1 + A_2 + A_3 = 1$; ϕ_1 is in μs.

Early decays (ϕ_1) are consistent with fluorescence results (Mendelson et al. 1973, Biochem. 12, 2250). Our observation of a 2.6 μs component (not detectable by fluorescence) implies that myosin's 400 ns motion is restricted in amplitude. This feature is not consistent with a free swivel model for S-1 attachment. Both amplitudes and rates of head motion are reduced in filaments. We applied the diffusion-in-a-cone model (Kinosita et al. 1977, Biophys. J. 20, 289) separately to fast and slow motions of myosin and filaments. Resulting rates (diffusion coefficients) and amplitudes (half cone angles) are: myosin fast motion: 360,000 s^{-1}, 44°; filaments, fast: 180,000 s^{-1}, 42°; filaments, slow: 26,000 s^{-1}, 40°. Results are consistent with probe parallel, but not perpendicular, to the long axis of S-1. Optical results were used to calculate EPR lineshapes and effective correlation times for restricted diffusion models. Calculations compared well with EPR results on myosin spin-labeled at the same site.

W-AM-Min2-4 FLUORESCENCE POLARIZATION STUDIES OF THE CONTRACTILE MECHANISM

Robert Mendelson, C.V.R.I. and Biochem./Biophys., Univ. of California, San Francisco, CA 94143

Time-resolved depolarization of fluorescence from the fluorophore 1,5 IEADANS attached to myosin heads has indicated that the heads possess considerable segmental flexibility. However, when myosin is aggregated into synthetic filaments or when in relaxed native myofibrils, the depolarization is much slower. This decrease in apparent rotational diffusion constant could be caused by either a decrease in the angular range available for head diffusion or by a true decrease of the diffusion constant without steric hindrance. Oriented EPR experiments (Thomas & Cooke, Biophys. J. (1980), 32, 891) favor the latter possibility as they have failed to detect any order in relaxed glycerinated muscle. Wilson and Mendelson (J. Mus. Res. and Cell. Mot., 1983, in press) have studied fluorescence polarization from chemically skinned psoas fibers labelled with 1,5 IAEDANS. They conclude, in agreement with X-ray diffraction results, that some order is present in relaxation. An examination of these results and those of Yanigida (J. Mol. Biol. (1981), 146, 539) using both a model of a random plus helical fraction and a model in which the cross-bridge is distributed (in 3D) about a mean orientation, indicates that the average dipole orientations are near ($\Delta\Theta_{dipole}<15°$) those found in rigor muscle. Since the two fluorophores used in these studies are located at two different myosin sites (nucleotide binding and SH_1) and since they have different dipole orientations (near 65 deg. and 30 deg.), these results suggest that the cross-bridge orientations in rigor and relaxation are similar.

Supported by N.I.H. grant HL-16683 and by N.S.F. grant PCM-7922174.

W-AM-Min2-5 ELLIPSOMETRY STUDIES OF RELAXED, RIGOR AND ACTIVATED SINGLE MUSCLE FIBERS.

Y. Yeh and R. J. Baskin, Depts. of Applied Science and Zoology, Univ. of Calif., Davis, Calif.95616

Optical ellipsometry measurements conducted on the single muscle fiber diffraction signals have yielded spectra which are sensitive to the state of the fiber. The linearly polarized light field vector, which at incidence is oriented 45° to the fiber axis, becomes elliptically polarized when collected at the diffraction orders. The characteristic ellipticity spectra exhibit changes upon passive stretch of an intact fiber, chemically induced relax-rigor transition in a skinned fiber and calcium induced activation (pCa = 6.65) of a relaxed skinned fiber.

Ellipticity spectra changes observed are characteristic of either orientational changes of intrinsically anisotropic fiber elements or arrangement changes of isotropic fiber elements (form birefringence). Observation of these spectra at diffraction orders allows us to further specify that the contributing elements are indeed of sarcomeric periodicity.

We have observed phase angle decrease consistent with the idea that orientational changes of anisotropic sarcomeric elements are the major source of ellipticity change in passive stretch and relax-rigor transition. The most likely candidate for these changes is the motion of the S-2 moiety of HMM. Recent studies on fibers undergoing calcium induced isometric tension show substantially different ellipsometric spectra. The ellipsometric phase angle increased upon calcium activation. These results will be discussed in relation to proposed crossbridge motion.

W-AM-A1 THERMOLUMINESCENCE FROM THE REACTION CENTER CHLOROPHYLL PROTEIN COMPLEX, CP47

H.Y. Nakatani[1], Govindjee[2] and Y. Inoue,[3] Intr. by T. Wydrzynski [1]MSU-DOE Plant Research Lab., Michigan State Univ.,[2] Biophys. Dept., Univ. of Illinois,[3] RIKEN, Saitama, Japan

The chlorophyll(chl) a-binding protein associated with the reaction center(P680-Pheophytin, Pheo) of photosystem II (PS II) has been characterized. The chl-protein was obtained by subjecting an glucopyranoside extract enriched in the chl-proteins of PS II to non-denaturing LDS-PAGE (4°C), (H.Y. Nakatani, 1983, in The Oxygen-Evolving System of Photosynthesis, eds. Y. Inoue et al. A.P. Tokyo, 49-54). The chl-a protein, denoted CP47, with an apoprotein molecular weight of 47 kilodaltons, elicited a chlorophyll fluorescence emission band at 695 nm upon illumination (77°K). Spectrophotometric analysis of CP47 (20°C) using a diode array rapid scanning spectrometer(DARSS) allowed us to resolve the light induced transients spectrally into a largely irreversibly bleached component with an absorption maximum at 679 nm and a small reversible component with an absorption maximum at 683 nm (Pheo). Room temperature fluorescence from CP47 could be quenched upon strong illumination in the absence of dithionite. This latter result was interpreted as arising from the formation of $Pheo^-$ (Klimov et al., 1977, FEBS Lett. 82, 183-186). The quenching of fluorescence (-dithionite) indicates to us that the primary acceptor, Q_A, of PS II is absent. With the isolation of CP47 and its characterization, direct thermoluminescent(TL) bands from the reaction center could be studied. In CP47, a new TL band at -70°C was observed; this band most likely arises from the recombination of the Z^+Pheo^- species. In a PS II core complex containing Q_A, another TL band was observed at -50°C which most likely arises from the recombination of the $Z^+Q_A^-$ species.

W-AM-A2 EVIDENCE FROM THERMOLUMINESCENCE FOR BICARBONATE ACTION AT QUINONE Q_B OF PHOTOSYSTEM II

Govindjee, H.Y. Nakatani, and Y. Inoue, Departments of Plant Biology and Physiology & Biophysics, University of Illinois, Urbana, IL 61801, MSU-DOE Plant Research Laboratory, Michigan State University, East Lansing, MI 48824, and RIKEN, Wako-Shi, Saitama-351, Japan.

Bicarbonate (HCO_3^-) addition to HCO_3^--depleted thylakoids is known to stimulate electron flow from the primary quinone acceptor, Q_A, of photosystem II (PS II) to the plastoquinone (PQ) pool. Thermoluminescence (TL) is known to be a probe, among other reactions, of the recombination of S_2 with Q_A^- or Q_B^-, where S_2 is the state of the O_2-evolving system produced by one flash (assuming that the majority of the S-states are in S_1 in darkness) and Q_B is the secondary quinone acceptor of PS II. Studies on the effects of HCO_3^--depletion on the TL of the thylakoids, following continuous saturating orange light, or a series of single saturating xenon flashes, have revealed (1) a 6 to 10°C shift of the $S_2Q_B^-$ TL band towards the higher temperature; (2) a reduction in the intensity of this TL band upon prolonged depletion; and (3) elimination after first few flashes of the characteristic period 4 oscillations in the intensity of this TL band as a function of flash number. The addition of HCO_3^-, even after 2-3 hours of HCO_3^- depletion, restores the TL characteristics to that of the control. Furthermore, addition of diuron, which blocks electron flow from Q_A^- to Q_B, produces a band due to $S_2Q_A^-$ recombination in both HCO_3^- depleted and reconstituted samples. These results allow us to suggest that HCO_3^--depletion (1) first increases the activation energy (Devault, Govindjee and Arnold, PNAS 80: 983-987, 1982) for $S_2Q_B^-$ recombination, and then decreases its rate; and (2) inhibits the cycling of the $S_2Q_B^-$ and $S_3Q_B^-$ recombination by inhibiting reactions at the Q_B-apoprotein. Thanks are due to A.W. Rutherford for discussions.

W-AM-A3 THE ELECTRON TRANSFER RATE FROM Q_A^- to Q_B IN IRON-DEPLETED RCs FROM R. SPHAEROIDES R-26.

R. J. Debus, M. Y. Okamura, and G. Feher, U.C.S.D., La Jolla, CA 92093.

The procedures developed to remove iron from RCs also cause dissociation of the H-subunit (1). The results obtained with these procedures may, therefore, not be characteristic of intact RCs (2). To overcome this problem, we prepared Fe-depleted RCs by reassociating H-subunits with LM containing < 0.05 Fe/LM. The resulting RCs (i.e., LMH complexes) retained 60-70% of the primary photochemical activity. They contained 0.18 ± 0.04 Fe/RC (determined by atomic absorption) but only ~ 0.03 Fe/RC were associated with the native binding site (determined from the EPR signal of $Q_A^-Fe^{2+}$). The rate of electron transfer from Q_A^- to Q_B (k_{AB}) was determined by varying the time interval between two laser flashes and measuring the amount of cyt $^{2+}$ oxidized after the second flash (3). The data (see Fig.) show that electron transfer from Q_A^- to Q_B proceeds in Fe-depleted RCs, although at a somewhat slower rate. The transfer was inhibited by o-phenanthroline and terbutryne. Thus, Fe^{2+} does not seem to play an obligatory role in the electron transfer from Q_A^- to Q_B.

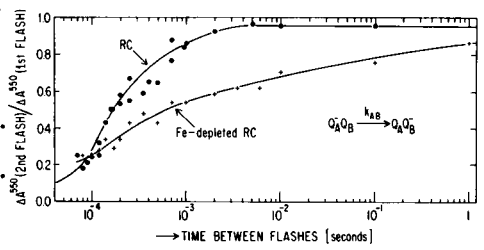

Work supported by grants from NSF and NIH.

1. R. J. Debus, M. Y. Okamura, and G. Feher (1981) Biophys. J. 33, 19a.
2. R. E. Blankenship and W. W. Parson (1979) Biochim. Biophys. Acta 545, 429-444.
3. W. W. Parson (1969) Biochim. Biophys. Acta 189, 384-446.

W-AM-A4 CHARGE RECOMBINATION KINETICS IN REACTION CENTERS WITH ANTHRAQUINONE AS THE PRIMARY ACCEPTOR: EVIDENCE FOR PROTONATION ACCOMPANYING THE FORMATION OF $D^+Q_A^-$. D. Kleinfeld, M. Y. Okamura and G. Feher, U.C.S.D., La Jolla, CA 92093.

Light absorbed by reaction centers (RCs) leads to a charge separation between the donor (D) and the primary quinone acceptor (Q_A), forming $D^+Q_A^-$. While redox titrations show that Q_A^- associates with a proton (pK = 9.8), optical (2) and EPR (3) measurements indicate that the proton is not directly bound to Q_A^-. To probe this protonation, we studied the recombination kinetics of $D^+Q_A^-$ with anthraquinone (AQ) replacing the native ubiquinone (UQ) in RCs from R. sphaeroides R-26. With AQ, as opposed to UQ, the recombination rate (k_{AD}^{obs}) is sensitive to small perturbations in the energy of Q_A^- (4,5). The recombination followed first order kinetics at all pH's, implying that the protonation occurred rapidly compared to k_{AD}^{obs}. The pH dependence of k_{AD}^{obs} (see Fig.) was modeled by a weighted average of the limiting rates at low and at high pH. The pK occurred at 9.8, the same as found by redox titrations. We interpreted the pH dependence of k_{AD}^{obs} as being caused by the rapid ($t \ll 10^{-2}$s) binding of a proton to a site near Q_A^- in response to the formation of $D^+Q_A^-$. Work supported by grants from the NIH and the NSF.

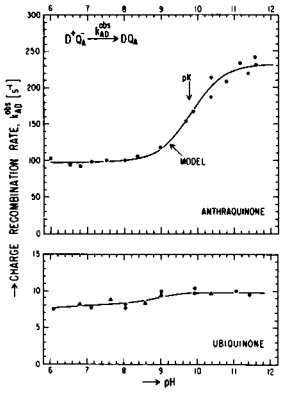

1) C. A. Wraight (1981) Israel J. Chem. 21, 384. 2) A. Vermeglio and R. K. Clayton (1977) B.B.A. 461, 159. 3) B. J. Hales and E. E. Case (1981) B.B.A. 267, 222. 4) M. R. Gunner et al. (1982) in Function of Quinones ... (Trumpower, ed.), Acad. Press, 222. 5) A. Gopher et al. (1983) Biophys. J. 41,121a.

W-AM-A5 CRYSTALLIZATION OF REACTION CENTERS FROM R. SPHAEROIDES R-26. J. Allen and G. Feher, U.C.S.D., La Jolla, CA 92093.

Recently, several integral membrane proteins have been crystallized (1,2,3), including the reaction center from R.viridis (2). Motivated by the more detailed characterization and smaller size of RCs obtained from R. sphaeroides, we have crystallized that system by two methods developed by Michel (2) and Garavito, et al. (3), respectively:

1) Small amphipatic molecules [1,2,3 - heptane triol (2.5%) and triethylammonium phosphate (3%)] were included with RCs (5.5 mg/ml) in LDAO (0.1%) and $(NH_4)_2SO_4$ (1.2M) at pH 7.0 and T = 23°C. Concentration by vapour diffusion against 2.1M $(NH_4)_2SO_4$ produced crystal habits A and B (see Fig.) Lowering the triol concentration triol to 1% resulted in crystal form C.

2) RCs were extracted and purified in β-octyl-glucoside (β-OG). In the presence of polyethylene glycol (PEG) and NaCl, phase separation occurs. The following protein solution: [RC] = 3.3 mg/ml, 0.8% β-OG, 0,25M NaCl,8% PEG, 15 mM Tris pH 8, was concentrated against 25% PEG and 0.8 M NaCl at T = 23°C. Crystal forms D, E, and F (see Fig.) grew in the detergent rich phase. Work supported by grants from the NSF and the NIH.

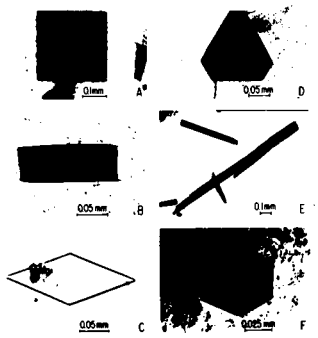

(1) H. Michel & D. Oesterhelt (1980) Proc. Natl. Acad. Sci. (US) 77, 1283; T. Ozawa, H. Susuki, & M. Tanaka (1980) Proc. Natl. Acad. Sci. (US) 77,928. (2) H. Michel (1982) J. Mol. Biol. 158, 567. (3) R. M. Garavito, J. Jenkins, J. N. Jansonius, R. Karlsson, and J. P. Rosenbush (1983) J. Mol. Biol. 164,313.

W-AM-A6 SINGLE CRYSTAL STUDIES OF REACTION CENTERS FROM R. SPHAEROIDES R-26. J. P. Allen, R. A. Isaacson, A. McPherson,‡ and G. Feher, U.C.S.D., La Jolla, CA 92093.

Crystals of reaction centers (RCs) described in the previous abstract were characterized by X-ray diffraction, EPR, and optical spectroscopy. X-ray data were obtained on two different crystal forms (see Figs. E and A of previous abstract). The first was established as P2 with β = 105°, a = 70 Å, b = 105 Å, c = 85 Å; it diffracted to 3.5 Å at 17°C (see Fig.1) and has 2 proteins/unit cell.

Fig.1

The latter form was tentatively identified as C222 with a = 185 Å, b = 168 Å, and c = 105 Å, and 8 proteins/unit cell. It exhibited a light-induced EPR signal (see Fig.2) having a line width and g-value corresponding to the oxidized donor D^+ (1). The g-anisotropy was determined to be $g_\perp - g_\parallel = (2.4 \pm 0.4) \times 10^{-4}$. Averaging of the EPR signal from the 8 proteins/unit cell reduces this value from the maximum predicted from frozen solution data (7×10^{-4}) (1). The optical spectra of the crystals, measured with a microspectrophotometer system, exhibited the characteristic absorption bands of frozen solutions with the additional feature of strong dichroism. Work supported by grants from the NSF and NIH.

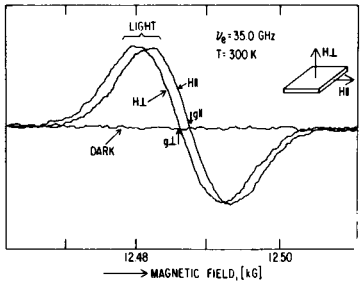

Fig.2

‡ University of California, Riverside.

(1) J. D. McElroy, G. Feher, and D. C. Mauzerall (1972) Biochim. Biophys. Acta 267, 363-374.

W-AM-A7 CHARACTERIZATION OF REACTION CENTERS CONTAINING Mn OR Zn IN PLACE OF Fe. M. Y. Okamura E. C. Abresch, R. A. Isaacson, and G. Feher. U.C.S.D., La Jolla, CA 92093.

Reaction centers containing appreciable amounts of either Mn or Zn in place of Fe (0.7 Mn, 0.2 Fe, 0.1 Zn) and (0.3 Zn, 0.6 Fe, 0.1 Mn) were prepared from R. sphaeroides R-26 grown in a medium of low Fe content (0.07 ppm) that was enriched in Mn or Zn (20 ppm). (1,2) The electron transfer rate from Q_A^- to Q_B , k_{AB} , was measured optically at 774 nm (pH 8). In the Mn enriched sample k_{AB}^{-1} was found to be the same (160 μs) as that measured in Fe containing samples. (3) Similarly, the binding constant of the electron transfer inhibitor o-phenanthroline was found to be the same in both samples. The Zn enriched RCs were monitored by EPR at 35 GHz where characteristic semiquinone signals (4) due to Q_A^- and Q_B^- were observed, showing that Zn had replaced Fe. RCs in the state $Q_A^-Q_B^-$ were created by illuminating RCs in the state $Q_AQ_B^-$ at cryogenic temperatures. An additional structure was observed in the spectrum of $Q_A^-Q_B^-$ that has been tentatively attributed to a magnetic interaction between Q_A^- and Q_B^-.

Work supported by grants from the NSF and NIH.

(1) G. Feher, R. A. Isaacson, J. D. McElroy, L. C. Ackerson and M. Y. Okamura (1974) B.B.A. 368,135.
(2) K. F. Ferris, V. Petrouleas and G. C. Dismukes, Abstract, ACS Meeting, Washington D.C., Aug.1983
(3) A. Vermeglio, R. P. Clayton (1977) B.B.A. 461, 159.
(4) G. Feher, M. Y. Okamura and J. D. McElroy (1972), B.B.A. 267, 222.

W-AM-A8 MAGNETIC FIELD DEPENDENCE OF THE LIFETIME OF P^F IN QUINONE CONTAINING BACTERIAL REACTION CENTERS, M.R. Wasielewski and P. Gast, Chemistry Div., Argonne National Laboratory, Argonne, IL 60439

We have measured the lifetime of the primary radical pair state P^F in bacterial reaction centers from R. sphaeroides R-26 and from R. viridis as a function of magnetic field. In each case the endogenous quinones in the reaction centers were present and chemically reduced. The observed magnetic field effects will be compared to those obtained from R. sphaeroides reaction centers which have their quinones removed. The presence of the additional unpaired electron spin in the reaction centers with quinones reduced has pronounced effects on the magnetic field dependent properties of the primary radical pair. Time resolved optically detected magnetic resonance spectra of these reaction centers will also be presented. These spectra will be discussed in terms of possible structural features of the reaction center that differ between R. sphaeroides and R. viridis.

This work was supported by the Division of Chemical Sciences, Office of Basic Energy Sciences, US DOE.

W-AM-A9 A pH DEPENDENT MIDPOINT POTENTIAL FOR THE SECONDARY QUINONE ACCEPTOR OF Rp. viridis R. J. Shopes and C. A. Wraight, Univ. of Illinois, Urbana, IL 61801.

The photosynthetic reaction center from Rp. viridis utilizes menaquinone as the primary quinone (Q_A) and ubiquinone as the secondary quinone (Q_B) of a two electron gate...

$$c\ c\ P\ Q_A\ Q_B \xrightarrow{h\nu} c\ c\ P^+\ Q_A^-\ Q_B \longrightarrow c^+\ c\ P\ Q_A^-\ Q_B \underset{}{\overset{K}{\rightleftharpoons}} c^+\ c\ P\ Q_A\ Q_B^-$$

$$c^+\ c\ P\ Q_A^-\ Q_B \xrightarrow{h\nu} \text{no cyt c oxidized}$$

$$c^+\ c\ P\ Q_A\ Q_B^- \xrightarrow{h\nu} c^+\ c\ P^+\ Q_A^-\ Q_B^- \longrightarrow c^+\ c^+\ P\ Q_A\ Q_B^=$$

The amount of bound cyt c_{558} oxidized on the second flash, relative to the first, is equivalent to the proportion of reaction centers in the Q_B^- state and from this we calculate K. The observed decrease of K with increasing pH, above the pK of 7.8 for Q_A (1), we interpret as a lower redox midpoint potential (Em) for Q_B^-/Q_B. Quantitatively the E_m of Q_B^-/Q_B decreases 60mV/pH between pH 9-11. However Q_B^- is not directly protonated as its spectrum is typical of an anionic semiquinone. A pH dependent E_m for Q_B may be explained by protonation of the protein residues. (1) Prince et al. BBA 440 (1976) 622-636. Supported by NSF PCM 80-12032.

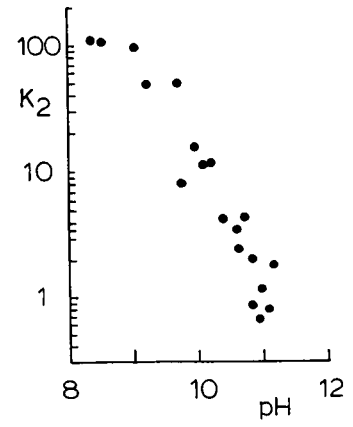

W-AM-A10 QUANTITATIVE ISOLATION OF THE LIGHT-HARVESTING COMPLEX B870 FROM R. RUBRUM AND ITS REVERSIBLE CONVERSION INTO A B820 FORM. P.A. Loach, J.F. Miller, S. Hinchigeri, P.S. Parkes and P.M. Callahan, Dept. Biochemistry, Molecular Biology and Cell Biology, Northwestern University, Evanston, IL 60201.

We have previously developed methodology for the isolation of a photosynthetic unit from R. rubrum which consisted of a high integrity reaction center-antenna complex (1). In an extension of this work, we have sought ways to reversibly separate the antenna complex from the reaction center while maintaining a quantitative yield of each. Our strategy developed over the last several years has been to first wash membrane vesicles free of all protein components except the PSU by a Triton X-100/EDTA wash step (2), lyophilization, benzene extraction of carotenoids (this step may be skipped for membrane vesicles from the G-9 mutant), and then to convert the remaining PSU into separated LH and RC complexes by a judicious choice of the concentration of octylglucoside. In this procedure we have found that the B870 LH complex is converted to a B820 complex, a process that is easily quantitatively reversed by cooling the sample or diluting with water. Since we felt that these latter treatments probably resulted in a reassociation of smaller subunits, it seemed likely that the assumed dissociated B820 form would be easily separated from the RC. Accordingly, we subjected the mixture of B820 form and RC's to gel filtration and successfully separated the LH complex and the RC in quantitative yield. Biochemical and spectroscopic characterization of the LH complex will be presented. (1) Loach, P.A., Hadsell, R.M., Sekura, D.L. and Stemer, A. (1970) Biochemistry 9, 3127. (2) Hall, R.L., Chu Kung, M., Fu, M., Hales, B. J. and Loach, P.A. (1973) Photochem. Photobiol. 18, 505.

W-AM-A11 DETERMINATION OF THE REGION OF THE TRIAZINE BINDING PROTEIN LABELED BY AZIDOATRAZINE Paul K. Wolber and Katherine E. Steinback, Advanced Genetic Sciences, 6701 San Pablo Ave., Oakland, CA 94608

It is known that triazine herbicides inhibit photosynthetic electron transport via direct interference with the function of the quinone Q_B, the second stable electron acceptor at the reducing side of photosystem II (PS II). From studies with the photoaffinity triazine analog, ^{14}C-azidoatrazine, it has been shown that binding occurs at a chloroplast membrane protein with a molecular weight (MW) of 32-34 kilodaltons (kDal). Studies of highly purified PS II preparations have demonstrated that this protein is a component of the PS II complex; analysis of partial tryptic digests of radiolabeled thylakoid membranes have shown that this protein is identical to the rapidly turned over 32-34 kDal protein of chloroplast thylakoids. We have photoaffinity labeled spinach thylakoid membranes with ^{14}C-azidoatrazine in vitro and/or with an assortment of ^{3}H-amino acids in vivo. The labeled protein has been isolated and cleaved with trypsin. The resulting fragments have been separated by gel filtration in organic solvent and the peptide pattern has been interpreted using the known gene sequence for the triazine binding protein. Over 80% of the ^{14}C-activity migrates as two peaks: one at the void volume (undigested protein) and the other at an apparent MW of 8.35$\pm$.76 kDal. The remaining activity migrates with the void volume (free azidoatrazine). The tryptic peptide covalently labeled by ^{14}C-azidoatrazine is most probably the fragment Pro-141 to Arg-225 (8.93 kDal), although the fragment Glu-65 to Arg-129 (7.05 kDal) cannot yet be fully discounted. More detailed mapping results and a discussion of the identified binding site location in relation to single amino acid changes involved in herbicide resistance will be presented.

W-AM-A12 ACTIVE AND RESTING CONFORMATIONS OF THE PHOTOSYNTHETIC O_2 EVOLVING COMPLEX. Gary W. Brudvig, Warren F. Beck and Julio dePaula, Dept. of Chemistry, Yale University, New Haven, CT 06520.

The S_2 state associated with O_2 evolution has been shown to exhibit a multiline EPR signal (Brudvig et al, 1983,BBA,723, 366). We find two distinctly different multiline EPR signals from the S_2 state in spinach PSII membranes depending on the length of dark adaptation prior to generation of the S_2 state. Extensively dark adapted samples exhibit a large multiline EPR signal, whereas, samples that are only dark adapted for two min. exhibit a relatively weak multiline EPR signal with substantial splitting of each hyperfine line. In extensively dark adapted samples the multiline EPR signal is not altered by D_2O substitution, 50 mM NH_4Cl, 40 μM NH_2OH, or even by Cl^- depletion. In light-activated samples all of the above treatments alter the multiline EPR signal from the S_2 state and Cl^- depletion, in particular, causes gross changes in the multiline EPR signal. Reconstitution of Cl^- depleted samples with Cl^- restores 95-100% of the activity and also restores the EPR properties of the untreated samples. These results suggest that the O_2-evolving complex from spinach can exist in two conformations. The resting conformation is formed upon long dark incubation and contains a Mn site that is insensitive to several treatments that block O_2 evolution. The active conformation is formed by illumination at room temperature and contains a Mn site that is open to interaction with water, amines, and halides. (Supported by USDA-CRGO, the Searle Scholars Fund, the Dreyfus Foundation, Research Corporation, the Petroleum Research Fund, and a NSF graduate fellowship to WFB.)

W-AM-B1 MATRIX FORMULATION OF THE TRANSITION FROM A STATISTICAL COIL TO AN ANTIPARALLEL β SHEET. Wayne L. Mattice, Department of Chemistry, Louisiana State University, Baton Rouge, Louisiana 70803, and Harold A. Scheraga, Baker Laboratory of Chemistry, Cornell University, Ithaca, New York 14853

A tractible matix formulation has been developed for the conformational partition function describing the formation of antiparallel β sheets. The formulation is applicable to chains with a finite degree of polymerization. Individual sheets may contain any number of strands, the number of residues in a strand may range upward from two, and no artificial constraint links the numbers of residues in neighboring strands. The weighting scheme uses one parameter (t) which is associated with every residue in the sheet, a second parameter (τ) associated with each residue that does not have a partner in a preceeding strand, and a third parameter (δ) associated with each β bend. While the formulation can easily be extended to treat specific-sequence heteropolypeptides, the initial emphasis is on implications for homopolypeptides. These implications are illustrated by numerical results obtained with several illuminating cases. Conditions are described which lead to the formation of different types of sheets: (1) "sheets" comprised of isolated extended strands, (2) cross-β fibers in which a sheet contains a large number of very short strands, (3) fibers in which a few very long strands run parallel to the fiber axis, and (4) sheets comprised of several strands in which the average strand contains five residues. The last type of sheet resembles those found in many globular proteins. It is formed when τ and δ are both small, with the ratio τ/δ being slightly less than one.

W-AM-B2 A"KNOTS"and"MATRICES" MODEL FOR GLOBULAR PROTEINS. Rufus Lumry & Roger Gregory, Dept. of Chemistry, U of Minnesota, U.S.A., and Carmel Jolicoeur, Dept. of Chem., U. of Sherbrooke, Canada.

On the basis of physical properties globular proteins fall in a unique class of solids; e.g. the temperature derivative of the heat capacity up to 55° is that characteristic of micelles but the compressibilities are those of respectable solids. Hydrogen-exchange data identify micelle-like matrices which exchange slowly and very slowly exchanging cores. Recent elegant studies of specific-site hydrogen-exchange behavior reveal "knots" of varying size and construction embedded in a soft matrix. The high cohesive energy of the dense knots must be a consequence of synergistic cooperation between well-organized peptide dipoles and adjacent aliphatic and aromatic sidechains which reduces the electrostatic energy. The knots do not contribute much thermodynamic stability but apparently determine the unfolding kinetics and the fluctuations available to the matrix as well as the low compressibility values. Knots exchange protons through local disruption except at temperatures near melting. The activated complex for unfolding is formed by cooperative swelling of one or more knots. In hydrogen exchange matrices and knots exhibit linear compensation behavior between $\Delta H^{\ddagger}$ and $\Delta S^{\ddagger}$ with characteristic T_c ranges (400-450K for matrices, 320-350K for knots). Linear enthalpy-entropy compensation behavior in proteins is usually the reflection of advancement in an unmeasured process through the measured process to which it is linked in a non-obligatory way. Such appears to be the case here since the same T_c values are observed in other measured processes; e.g. T_c of 330K for thermal unfolding rates, T_c of 400K in bond-rearrangement steps of chymotryptic catalysis. The limited data available for enzymic processes demonstrate steps in both T_c ranges as well as enzyme-substrate association with low T_c values closer to those found in hydrophobic hydration. Supported by NIH PO116833 NSFPCM8003744 and National Science and Engineering Research Council of Canada.

W-AM-B3 PROTEIN CONFORMATION ENERGY MINIMIZATION WITH STATISTICALLY DERIVED SECONDARY STRUCTURE PARAMETERS. R. L. Jernigan and S. Miyazawa, Lab. of Math. Biol., NCI, NIH, Bethesda, MD 20205

Applications of dynamic programming provide means for minimizing the energies of secondary structures. In a generalization of our previous method [Jernigan and Szu, Macromolecules 12, 1156, 1979], we have developed a more general method to account for interactions up to any specified range of interaction along the chain. As input to this method we have collected data from a set of globular protein crystal structures; this set of proteins has been carefully selected on the basis of consistency of their intra-residue geometries. The relatively small number of high quality crystal structures imposes serious limits to the collection of requisite statistical parameters. We have collected statistics for various types of pairs, for neighbor dependences of various ranges. Approximate expressions for higher order groups of residues based on these pairwise probabilities are tested by comparing against the occurrences of higher order groups in the protein sample. Convergence of the pair probabilities to the single probabilities with increasing range of separation has been investigated to determine interaction ranges. Also we have attempted to look systematically at 1) the dependence of a central residue's conformation on the backbone conformations of its neighbors, corresponding to backbone-backbone and backbone-central side chain interactions and 2) the dependence of the conformation of a central residue on the amino acid types of its neighbors, corresponding to average central backbone-side chain and side chain-side chain interactions.

W-AM-B4 FOLDING PATHWAY OF A CIRCULAR FORM OF BOVINE PANCREATIC TRYPSIN INHIBITOR (BPTI). David P. Goldenberg and Thomas E. Creighton. Medical Research Council, Laboratory of Molecular Biology, Cambridge CB2 2QH England.

A circular form of BPTI has been prepared by linking the N- and C- termini, which are in close proximity in the native conformation, together in a peptide bond. The cross-linked protein can refold to the native conformation after the three disulphide bonds in the native protein have been reduced. The pathway of folding has been determined by isolating, identifying and determining the kinetic roles of intermediates contiaining disulphide bonds, as was done previously for the unmodified protein. The intermediates in the refolding of the circular protein are primarily the same as those for the unmodified protein. However, the cross-link does significantly alter the stabilities and rates of interconversion of some of the intermediates, and the quantitative differences between the proteins indicate the roles of the terminal regions of the unmodified protein during folding. The cross-link does not affect the over-all stability of the one-disulphide intermediates, but does promote the formation of the second disulphide bond, indicating that the termini are not brought together until the two-disulphide stage of the folding pathway. Surprisingly, the cross-link does not appear to greatly stabilize the native conformation, apparently because the native protein is slightly strained by the cross-link. These results demonstrate that the extent of stabilization of a protein by a cross-link depends on the effects on the native conformation, as well as on the effect on the entropy of the unfolded chain.

W-AM-B5 A VOLTAGE SWITCHABLE ION CHANNEL; MODELS AND MUTANTS OF COLICIN E1. C. Levinthal, R. Fine, C. Cleveland, F. Levinthal, Q.R. Liu. Depart. of Biol. Sci., Columbia Univ., NY, NY 10027

The bacterial toxin colicin E1 kills sensitive cells by forming an ion channel in the plasma membrane which releases the membrane potential, thereby stopping oxidative phosphorylation. The activity of this channel can be demonstrated in a Mondal black lipid membrane in which it can be switched on or off by changing the voltage across the membrane (Schein, et al. 1978. Nature 376: 159-163). The sequence of the 522 amino acids in colicin E1 is known from the DNA sequence of the gene which encodes it (Yamada et al. PNAS 79: 2827-2831). We have isolated a C-terminal fragment, after cyanogen bromide cleavage, which contains 152 amino acids and which has the same channel forming and voltage switchable properties as the intact molecule (Cleveland et al. 1983. PNAS 271: 3706-3710). The time for the voltage induced transition from OPEN to CLOSED or the reverse can be of the order of seconds. We take this to imply that a major conformational change is involved in the transition.

We have considered two classes of molecular models for the channel in the OPEN state. The first involves six alpha helices spanning the membrane with the lumen in their center. The second model makes use of a beta barrel structure to form the channel. In both models, salt-bridges facing the lipids are taken as stablizing interactions. Since the separation along the peptide chain is very different for salt-bridges which are possible in alpha helices or in beta sheets we can use this information for predicting the effects of altering individual amino acids. *In vitro*, site-specific, mutagenesis to alter the amino acid sequence of the peptide is being used to test specific models and to distinguish between masses of them. Results of the mutagenesis as well as a detailed discussion of the model will be presented. Supported by NIH grant RR00442.

W-AM-B6 KINETIC STUDIES SHOW Ca^{2+} AND Tb^{3+} HAVE DIFFERENT BINDING PREFERENCES TOWARD THE FOUR Ca^{2+}-BINDING SITES OF CALMODULIN. C.-L.A. Wang, P.C. Leavis and J. Gergely, Dept. of Muscle Res., Boston Biomed. Res. Inst., Dept. of Biol. Chem. and Neurology, Harvard Med. School, and Dept. of Neurology, Mass. Gen. Hosp., Boston, MA 02114

The stepwise addition of Tb^{3+} to calmodulin (CaM) yields a large tyrosine-sensitized Tb^{3+} luminescence enhancement as the third and fourth ions bind to the protein (Wang et al., Eur J. Biochem. 124 7, 1982). Since the only tyrosine residues in CaM are located within binding sites III and IV, these results suggest that Tb^{3+} binds first to sites I and II. Recent NMR studies have provided evidence that Ca^{2+}, on the other hand, binds preferentially to sites III and IV. Kinetic studies using a stopped-flow apparatus also show that the preferential binding of Ca^{2+} and lanthanide ions are different. Upon rapid mixing of Ca_2-CaM with 2 Tb^{3+}, there was a small and rapid tyrosine fluorescence change but no Tb^{3+} luminescence was observed, indicating that Tb^{3+} binds to sites I and II but not sites III and IV. When 2 Tb^{3+} are mixed with Dy_2-CaM, Tb^{3+} luminescence rises rapidly as Tb^{3+} binds to the empty sites III and IV, followed by a more gradual decrease ($k=0.4\ s^{-1}$) as the ions redistribute themselves over the four sites. These results indicate that (i) both Tb^{3+} and Dy^{3+} prefer binding to sites I and II of CaM, and (ii) the binding of Tb^{3+} to CaM is not impeded by the presence of 2 Ca^{2+} initially bound to the protein. Thus, the Ca^{2+} and lanthanide ions must exhibit opposite preferences for the four sites of CaM: sites III and IV are the high affinity sites for Ca^{2+}, whereas Tb^{3+} and Dy^{3+} prefer sites I and II. In the case of troponin-C (TnC) where Ca^{2+} and Tb^{3+} are known to compete for the same sites, addition of 2 Tb^{3+} to Ca_2-TnC results in a slow ($k=0.7\ s^{-1}$) increase of Tb^{3+} luminescence as the ion displaces bound Ca^{2+} from sites III and IV.

W-AM-B7 INFLUENCE OF CITRATE AND pH ON ALUMINUM-INDUCED CONFORMATIONAL CHANGES IN CALMODULIN. Charles Suhayda and Alfred Haug. Department of Botany and Plant Pathology, and Pesticide Research Center, Michigan State University, East Lansing, Michigan 48824.

The stoichiometric binding of aluminum ions to bovine brain calmodulin (CaM) has been demonstrated to cause both a loss of helix content and regulatory function of this protein (N. Siegel and A. Haug, Biochim. Biophys. Acta 744, 1983,36). Because of its pivotal regulatory role within the cell, protective mechanisms should exist that ensure the proper function of CaM. We have shown that citrate, a naturally occurring organic acid, can both protect CaM from undergoing a conformational change in the presence of aluminum and can partially restore aluminum-induced structural changes in the protein. Studies with the hydrophobic, fluorescent surface probe 8-anilinonaphthalene sulfonic acid (ANS) have shown that the addition of 10 citrate molecules per calmodulin, at pH 6.5, prior to titration with aluminum ions, can prevent an Al-induced fluorescence increase until aluminum ions are in excess of citrate molecules. Titration of CaM with calcium ions under identical conditions has shown that citrate did not affect the binding of calcium to CaM. As demonstrated in CD studies, the prior addition of excess citrate can protect the protein from an Al-induced loss of helix content. Following the addition of 3 aluminum ions per CaM, at pH 6.0 and 6.5, the addition of six citrate molecules decreased the Al-induced enhancement in hydrophobic surface area by about 50 percent, as judged by fluorescence intensity, whereas this decrease was 40 percent, at pH 7.0 and 7.5. CD data have shown that the Al-induced loss of helical content can only be partially restored by citrate. Thus, the presence of preexisting chelators can protect CaM from aluminum injury. A high chelator content may therefore provide cells with resistance to the toxic effects of aluminum ions.

W-AM-B8 MODIFICATION OF TROPONIN C WITH FLUORESCENT PROBES AFFECTS ITS BINDING TO THE OTHER TROPONIN SUBUNITS. Z. Grabarek, P.C. Leavis, T.Tao and J. Gergely. Dept Muscle Res., Boston Biomed. Res. Inst. and Dept. Neurology, Mass. General Hosp., Boston, MA 02114.

To obtain information about the binding between troponin subunits, we have utilized the exchange kinetics of a subunit carrying a fluorescent label with its unlabelled counterpart. From the extent of the exchange it appears that the binding constant of the labelled species (K^*) differs from that of the unlabelled one (K). The ratio, K^*/K, can be obtained by a curve fitting procedure applied to a plot of the fluorescence change vs the ratio of the unlabelled and labelled subunits. TnC was labelled with 1,5-IAEDANS at Cys-98 or with DANZ at Met-25. In the case of the TnC^{AEDANS}-TnI complex, values for the equilibrium binding constant, K^*, determined from fluorescence titration curves in the absence and presence of Ca^{2+} are 5.3×10^5 and 2.2×10^7 M^{-1}, respectively. For the same complex, $K^*/K = 0.18$ in the absence of Ca^{2+} and 0.015 in its presence. These values yield binding constants for the unlabelled complexes, $K = 3.0 \times 10^6$ ($-Ca^{2+}$) and $1.5 \times 10^9 M^{-1}$ ($+Ca^{2+}$). Thus, while Ca^{2+} increases the binding constant for the unlabelled TnC-TnI complex by a factor of 500, the increase for the labelled complex is only ~40-fold. This suggests that the probe at Cys 98 interferes with the TnC-TnI interaction at the Ca^{2+}-modulated site of TnC viz. residues 98-100 (cf Grabarek et al, 1981, J. Biol. Chem. 256; 13121). For TnC^{AEDANS}-TnT, $K^*/K=1.8$ in the presence of Ca^{2+} and 4.2 in its absence, indicating that the label slightly enhances the interaction. DANZ-labelled TnC exhibits enhanced binding to both TnI and TnT except in the case of TnC^{DANZ}-TnT in the presence of Ca^{2+} when $K^*/K=0.15$. These data show that labels can significantly affect binding parameters between proteins. Nevertheless, they may provide useful information about the role of the labelled region in complex formation.

W-AM-B9 STUDIES ON THE PROXIMITY RELATIONSHIPS BETWEEN THIN FILAMENT PROTEINS USING BENZOPHENONE-4-MALEIMIDE AS A SITE-SPECIFIC PHOTOREACTIVE CROSSLINKER. T. Tao, M. Lamkin, and C. Scheiner, Dept. of Muscle Research, Boston Biomed. Research Inst., and Dept. of Neurology, Harvard Medical School, Boston, MA 02114.

Previous work had shown that benzophenone-4-maleimide (BP-Mal) is an effective photoreactive crosslinker of protein moieties (Lamkin & Tao, Biophys. J. 37, 37a, 1982). In this work we report more extensive studies in which BP-Mal was used to specifically label 1) actin at Cys-374, 2) αα-Tm at Cys-190, and 3) TnC at Cys-98. We found that only a small amount of internally crosslinked species was formed when BP-G-actin was irradiated. For BP-F-actin, the extent of intra-subunit photocrosslinking was significantly increased, and only a small amount of inter-subunit photocrosslinking was detected. When BP-Tm was irradiated in the presence of troponin, photocrosslinking to all three subunits was detected, with the crosslinking yield decreasing in the order of TnT, TnI, and TnC. BP-TnC photocrosslinked to either TnI, or TnT in the binary complexes. Irradiation of the reconstituted ternary complex of BP-TnC, TnI and TnT produced both the BP-TnC.TnI and the BP-TnC.TnT crosslinking products. We conclude that 1) Actin polymerization changes the conformation of each subunit around Cys-374 in such a manner that the residue comes in more contact with the surface of the subunit. 2) The tertiary structure of troponin is such that that the other two subunits meet at the region near Cys-98 of TnC, and Cys-190 of Tm may also be in the vicinity. Recently proposed structural models for troponin are consistent with this conclusion. (Abbreviations: Tm, tropomyosin; TnC, TnI and TnT, troponin-C, -I and -T; BP-TnC etc., BP-Mal labeled TnC etc.) (Supported by NIH grant AM21673)

W-AM-B10 FLUORESCENCE LIFETIME AND ACRYLAMIDE QUENCHING STUDIES OF THE INTERACTION BETWEEN TROPONIN SUBUNITS. P. C. Leavis, E. Gowell and T.Tao, Dept. Muscle Research, Boston Biomed. Research Inst. and Dept. Neurology, Harvard Medical School, Boston, MA 02114.

Fluorescence lifetime and acrylamide quenching studies were carried out to characterize the interactions between the subunits of troponin under various conditions of metal ion binding. Troponin-C was labeled at Cys-98 with 1,5-IAEDANS. In the presence of Ca^{2+}, the fluorescence decay of IAEDANS-labeled troponin-C (TnC*) was mono-exponential, of lifetime τ=15.5 ns, and quenching rate constant k_q=2.97 x 10^8 $M^{-1}s^{-1}$. In the absence of Ca^{2+}, the decay was resolvable into a major component of τ=11.9 ns and a minor component of τ=20.5 ns, with corresponding values of k_q=4.80 x 10^8 and 0.66 x 10^8 $M^{-1}s^{-1}$, respectively. Upon the binding of either troponin-I (TnI) or troponin-T (TnT) in the presence of Ca^{2+}, τ increased to ~18 ns, and k_q decreased to ~0.8 x 10^8 $M^{-1}s^{-1}$. For the Ca^{2+} form of the TnI-TnT-TnC* ternary complex, values of τ=17.6 ns and k_q=1.73 x 10^8 $M^{-1}s^{-1}$ were obtained. These values did not vary significantly when Ca^{2+} was removed, or when Mg^{2+} replaced Ca^{2+}. These findings were interpreted as follows: the region around Cys-98 of TnC* adopts a looser conformation upon the removal of Ca^{2+} from the high affinity sites. Both TnI and TnT bind to TnC* in the region containing Cys-98. The probe is shielded from the solvent to a greater extent in the binary complexes than in the ternary complex. The lack of metal-induced changes in the ternary complex indicates that conformational changes in this region of the molecule, if they do occur, do not result in changes in the solvent accessibility of the probe. (Supported by NIH grants HL20464 and AM21673).

W-AM-B11 FLUORESCENCE LIFETIME AND ANISOTROPY STUDIES WITH LIVER ALCOHOL DEHYDROGENASE AND ITS COMPLEXES. Maurice R. Eftink and Karen Hagaman, Department of Chemistry, University of Mississippi, University, MS 38677.

We have measured the apparent phase and modulation fluorescence lifetimes of alcohol dehydrogenase at multiple modulation frequencies (6, 18, and 30 MHz) and have analyzed the data in terms of the individual lifetime and fractional intensity contributions of Trp 314 and Trp 15 of this protein. We find τ_{314} = 4.0, τ_{15} = 8.2 and f_{314} = 0.67, at 20°C, which is in general agreement with values reported by Ross etal using pulse-decay methodology (Ross etal, Biochemistry 20, 4369 (1981)). In ternary complexes formed between the protein, NAD^+, and either pyrazole or trifluoroethanol, we find the lifetime of Trp 314 to be reduced, indicating that the binding of these ligands causes a dynamic quenching of this residue. The lifetime of Trp 314 is reduced more in the trifluoroethanol ternary complex than that with pyrazole. Also, the alkaline quenching transition of alcohol dehydrogenase is found to result in a dynamic quenching of Trp 314. No significant change in lifetimes or fractional intensities of the two trp residues is found upon selective removal of the active site Zn^{+2} ions of this protein.

From studies of the fluorescence anisotropy of this protein as a function of added acrylamide (which selectively quenches the surface Trp-15 residues), we have determined the steady state anisotropy, r, of each residue to be r_{314} = 0.26 and r_{15} = 0.21. For the ternary complexes, the anisotropy of each residue increases slightly. The increase for Trp-314 is expected, since its lifetime is reduced upon NAD^+ binding, but the increase in r for Trp-15 indicates that the motional freedom of this residue is limited by the binding of ligands, even though Trp-15 is some distance from the active site. (This work was supported by NSF Grant PCM-82-06073.)

W-AM-C1 THE ROLE OF THE ELECTRICAL DOUBLE LAYER IN EXCITATION. Martin Blank, Physiology Dept. Columbia Univ., New York, NY 10032

The transient ionic fluxes associated with excitation are unusual in terms of the electrical potentials and ionic concentrations across the resting cell membrane. However, the relevant physical properties at the surfaces of the membranes (i.e. surface potential, surface concentration, surface capacitance) are generally quite different from the bulk values, and their behavior during transients should account for the fluxes. To study the contributions of ionic processes in the electrical double layers during transients, we have developed the Surface Compartment Model (SCM) approximation, which treats the surface layers as compartments. Differential equations for conservation of ions and charges, as well as for ion binding kinetics, are used to describe changes in the surface layers. A non-selective voltage-dependent increase in the permeability of the SCM membrane to cations, causes a peak inward current followed by a steady state outward current, as observed in a voltage clamp. Both currents depend upon the clamp voltage approximately as in the squid axon membrane. These results (Blank, Bioelectrochem. Bioenerg. 10:451, 1983) suggest that ionic processes in the electrical double layers at membrane surfaces cause the unusual ionic fluxes, and changes in the surface properties (e.g. surface charge, surface capacitance) may explain the effects of various chemical agents. Supported by Research Contract N00014-83-K-0043 from the Office of Naval Research.

W-AM-C2 STUDIES OF NERVES BY RAMAN SPECTROSCOPY. B. Simic-Glavaski, Chemistry Department and Case Center for Electrochemical Sciences, Case Western Reserve University, Cleveland, Ohio 44106.

Laser Raman spectroscopic observations were made on the walking leg nerves of the lobster (*Homarus americanus*) which contain large sensory and motor axons. The nerve bundles were also examined when the nerves were stained with photic probe molecules such as water soluble transition metal tetrasulfonated phthalocyanine (M-TsPc) that closely resembles a heme molecule.

Raman spectra obtained from the nerve bundles at various polarization potentials provide information at a molecular level. A detailed analysis of data obtained from M-TsPc under various experimental conditions are highly informative. Very intense resonant Raman and resonant Surface Enhanced Raman Spectra obtained from M-TsPc in aqueous solution phases and adsorbed at silver electrode interfaces provide the band assignment and analysis of physadsorbed behavior of macrocycle species under controlled electrode potential. However, the adsorbed M-TsPc on the nerve bundles indicate change in spectra and some chemical interaction. The spectral changes of the adsorbed M-TsPc on the nerve bundles are a function of the nerve polarization and suggest oxidation-reduction mechanism in the pyrrole ring. This experimental evidence was also obtained from the adsorbed M-TsPc on the silver electrode in the oxidation-reduction potential domains of the macrocycle molecules.

W-AM-C3 FAILURE OF THE USSING FLUX-RATIO EQUATION DOES NOT INVALIDATE ELECTRODIFFUSION MODELS. H. Richard Leuchtag, Department of Biology, Texas Southern University, Houston, TX 77004.

In order to develop physical theories of the intrinsic ion-conducting units (channels) of an excitable cell, it is essential to proceed from a lumped-circuit (Hodgkin-Huxley) model to a local one that permits the description of nonuniform electric fields.[1] For this, the electrodiffusion (ED) model, based on the Nernst-Planck equation, continuity equation and Gauss's law, is a reasonable candidate. However, a number of objections to ED have been raised, including one based on the Ussing-Teorell-Behn flux-ratio equation (FRE).[2] This argument states that, since data on isotopic potassium fluxes in axons are in contradiction to the FRE, which is derived from the Nernst-Planck equation, electrodiffusion models will not adequately describe the behavior of excitable cells. It should be noted, however, that the derivation[3] of the FRE depends on additional assumptions not required by ED models. These are (1) steady state and (2) special boundary conditions that in effect impose infinite electrochemical potential differences on the two isotopic ions. Since (1) and (2) are mutually contradictory, and (2) not realistic, the argument from the FRE does not constitute a decisive objection to ED models of excitable cells.

1. H.R. Leuchtag and H.M. Fishman, in Structure and Function in Excitable Cells (D.C. Chang, I. Tasaki, W.A. Adelman Jr. and H.R. Leuchtag, eds.), Plenum, NY, 1983.
2. B. Hille and W. Schwarz, J. Gen. Physiol. 72:409-442 (1978).
3. H.H. Ussing, Acta Physiol. Scand. 13:43-56 (1949).

W-AM-C4 A CALCIUM DIFFUSION MODEL PREDICTS FACILITATION, BUT NOT THE TIME COURSE OF TRANSMITTER RELEASE, DURING TETANIC STIMULATION. Robert S. Zucker, Physiology-Anatomy Dept., Univ. of Calif., Berkeley, CA 94720.

Calcium ions are believed to be directly responsible for transmitter neurosecretion during a presynaptic action potential, as well as synaptic facilitation following prior activity. A simple one-dimensional diffusion model has been described which accounts for the rapid termination of evoked release and the magnitude and time course of facilitation associated with a single spike, and the time course of average presynaptic calcium changes measured with arsenazo (J. Neurosci. 3:1263,1983).

I have extended this model to simulate the growth of facilitation during, and its decay following, a train of 100 spikes at 20 Hz. The model predicts accumulation of facilitation and the appearance of a slowly decaying process (augmentation) which closely resemble the behavior of frog neuromuscular junctions. However, the termination of transmitter release following highly facilitated action potentials is much too slow. Simulations in which buffering is saturable or unsaturable, calcium removal is by a membrane pump or by uptake into organelles, and local calcium influx is taken as high due to calcium channel clustering or low due to a uniform calcium channel distribution, all show similar behaviors.

Possibly an early rapid phase of 3-dimensional calcium diffusion away from discrete channel entry points can account for the discrepancy. Alternatetively, other factors, such as the voltage across the presynaptic membrane, may influence the rate of secretion during an action potential.

Supported by NIH grant NS 15114.

W-AM-C5 MODELLING OF SUBMEMBRANOUS CALCIUM-CONCENTRATION CHANGES AND THEIR RELATION TO RATE OF PRESYNAPTIC TRANSMITTER RELEASE IN THE SQUID GIANT SYNAPSE. S. M. Simon, M. Sugimori and R. Llinás. Dept. Physiol. & Biophys., New York Univ. Med. Ctr., 550 First Ave., New York 10016.

Rate of transmitter release is tightly coupled to the rate of Ca++ entry into the presynaptic terminal (Llinás et al., Biophys. J. 33, 1981). It has been assumed that localized changes in intracellular [Ca++] are responsible for triggering release. We used both analytical and numerical techniques to model the submembranous changes of [Ca++] during presynaptic depolarization and their relationship to rate of transmitter release. Different assumptions regarding intracellular buffering, the diffusion constant for Ca++, the packing of Ca++ channels in the plane of the membrane and the flux/channel were tested. Several conclusions are derived about the relation between Ca++ and release independent of these assumptions. First, the modelled intracellular changes that occur when a given channel opens are highly localized to the region of that channel. Second, as the presynaptic cell is depolarized from rest there is a decreased driving force for Ca++ and a decreased flux/channel, and thus a small depolarization produces a larger local increase of [Ca++] than does a large one. Third, models that assume the rate of release is a nonlinear function of [Ca++] predict a greater rate of release for small depolarizations than is actually observed. This is a direct consequence of the larger local changes of [Ca++] predicted for smaller pulses. Finally, if we assume that when a unitary release event occurs there is a delay of >500 μsec before release can occur at the same site, then a model for release with a linear dependence on [Ca++] predicts the proper rate of release and the observed voltage hysteresis and depletion of transmitter release in this synapse. [Supported by NS14014, NINCDS]

W-AM-C6 CALCIUM-ACTIVATED SLOW INWARD CURRENT IN APLYSIA BURSTING PACEMAKER NEURONS. Richard H. Kramer and Robert S. Zucker, Dept. Physiology-Anatomy, Univ. of Calif., Berkeley, CA 94720

Molluscan bursting pacemaker neurons exhibit depolarizing afterpotentials (DAPs) which follow both single action potentials and spontaneous bursts. The DAPs provide a mechanism for sustaining repetitive firing, and are critical for the depolarizing phase of bursting activity. Thompson (1976) and S. Smith (1978) have described the kinetics and voltage-sensitivity of a slow inward tail current (I_B) which generates the DAPs in bursting cells. We have further investigated the I_B tail current in Aplysia abdominal ganglion bursting neurons L2-L6 (axotomized) and R15 (intact).

The I_B tail current was elicited by brief (10-50 msec) depolarizing voltage-clamp pulses from a holding potential of -60 mV. The I_B tail current is supressed when the pulse potential approaches E_{Ca} (i.e. +120 mV) and is largest when the pulse potential results in a large Ca influx (i.e. +30 mV). The I_B tail is blocked by substitution of external Co or Mn for Ca, and by intracellular injection of EGTA. Therefore, the activation of I_B is Ca-dependent.

I_B is distinct from the Ca current which underlies the negative-resistance region of the steady-state I-V curve of pacemaker cells. The negative resistance current increases following EGTA injection and is unaffected by removal of external Na, while I_B is decreased by Na removal.

I_B appears to be identical to a Ca-activated inward current which has an E_{rev} of about -20 mV, which we elicited by injecting Ca into bursting neurons whose Ca-activated K current was blocked with 50 mM TEA. The Ca-elicited current is reduced by removing external Na or Ca; removing both ions shifts the E_{rev} to about -60 mV. Therefore, the current is probably carried by a mixture of Na, Ca, and K ions, similar to non-specific Ca-gated currents previously described in cardiac fibers, neuroblastoma, and snail neurons. [Supported by NIH grant NS 15114].

W-AM-C7 INTRACELLULAR FREE Ca^{2+} ACTIVITY IN BRAIN NERVE TERMINALS MEASURED WITH QUIN 2.
D.A. Nachshen, Department of Physiology, Cornell University Medical College, New York, NY 10021.

The intracellular free Ca^{2+} activity (Ca_i) in pinched-off presynaptic nerve terminals (synaptosomes) isolated from rat brain was measured with the fluorescent Ca indicator, Quin 2. Synaptosomes were loaded with Quin 2 by incubation with the permeant acetoxymethyl ester derivative of the indicator, which was subsequently hydrolyzed and trapped in the nerve terminals. The fluorescence signal from synaptosomes in solutions containing 145 mM NaCl, 5 mM KCl, and 0.1 - 1 mM $CaCl_2$, corresponded to a Ca_i of 0.2 - 0.3 μM. There was only a slight, 0.1 μM, increase in Ca_i when the external Na concentration was lowered by replacing 50 mM Na with choline, but Ca_i increased to more than 1 μM when the synaptosomes were depolarized, by replacing 50 mM Na with K. The level of Ca_i also increased to more than 1 μM when the synaptosomes were depolarized by the addition of veratridine, an agent that increases the Na conductance of the nerve terminals. The effect of veratridine on Ca_i was partially reversed after the addition of the Na channel blocker, tetrodotoxin. Ca_i was also increased to more than 1 μM when ouabain (1 mM) was added, or when all of the external Na was replaced by choline. The elevation of Ca_i produced by high K, veratridine, ouabain, and Na removal, was not observed in Ca-free solutions. These results indicate that synaptosomes are able to regulate Ca_i, and that this regulation can be conveniently studied with Quin 2.

Supported by an Investigatorship from the New York Heart Association, and NIH grant NS-16461.

W-AM-C8 GLOBAL DYNAMICS OF BRAIN AND ITS HIERARCHICAL OSCILLATING ELEMENTS
E. Basar(1), O. Gurel(2) and J. Roschke(1), (1) Institut fur Physiologie Medizinische Hochschule Lubeck, and (2) IBM Cambridge Scientific Center, Cambridge, MA.

In this communication a novel methodology to study the activities (dynamics) of the brain is presented. The approach is based on global interactions of the hierarchical oscillations which are experimentally (clinically) observable. Theoretical considerations (global analysis) are applied to the analysis of the $\alpha,\beta,\theta,\delta$ rhythms of brain to show these rhythms as interacting elements of the multidimensional dynamics. Specifically, two and three dimensional interaction have been experimentally observed and theoretically analyzed. The approach promises future extensions to both further understanding the behavior of central nervous system, and also identifying the elements of pathological aberrations.

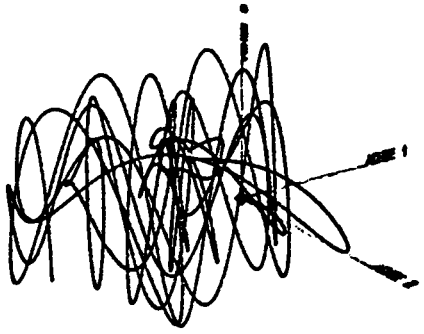

W-AM-C9 **HYDROGEN ION CURRENT IN AMBYSTOMA OOCYTES.** **M. E. Barish and C. Baud, Department of Physiology, UCLA School of Medicine, Los Angeles, California 90024.**

An outward current found in immature oocytes of the urodele amphibian Ambystoma was studied using the two microelectrode voltage clamp technique. The reversal potential of this current varied with the external pH, changing approximately 54 mV/unit between pH 6.9 and 8.4. The reversal potential was not affected by changes in $[K^+]_o$ and $[Cl^-]_o$, and was slightly sensitive to $[Na^+]_o$. These observations suggested that the outward current was an H ion current.

The voltage dependencies of conductance and kinetics were examined. At pH 7.4 the steady state conductance-voltage (g-V) relation was sigmoidal with membrane voltage. The time courses of activation and deactivation were proportional to $1-\exp(-t/\tau)$. A plot of time constant (τ) against voltage was bell-shaped, with a maximum near the voltage of half-maximum conductance. These were properties expected of a current gated by membrane voltage.

At higher $[H^+]_o$, the maximum activatable conductance ($\bar{g}$) was increased for both outward currents and inward tail currents, a result consistent with H^+ being the permeant ion. Raising $[H^+]_o$ also decreased the steepness of the voltage sensitivity of the g-V relation, suggesting an interaction between H ions and the current gating mechanism.

Increasing $[H^+]_o$ shifted the g-V and τ-V relations towards positive voltages. As a result, inward current was not observed at voltages more negative than the reversal potential. This 'pH-compensation' of channel gating in the direction of internal alkalinization might be of adaptive value if the H ion current has any relation to the reductions in $[H^+]_i$ that are seen at maturation and fertilization of amphibian eggs.

W-AM-C10 FERRITIN AS A PROBE IN EM AND EDAX STUDIES OF THE DIFFUSION CHARACTERISTICS OF THE SQUID GIANT AXON SHEATH COMPLEX. A. J. Hodge and W. J. Adelman, Jr., Laboratory of Biophysics, NINCDS, NIH at the MBL, Woods Hole, MA 02543.

The squid giant axon sheath includes a single layer of "interdigitating" Schwann cells (SC) in contact with the axolemma and one another, but not forming tight junctions. These cells are surrounded closely by a basement lamina (BL). Additional collagen layers, alternating in direction, together with interspersed fibroblasts, form the remainder of the sheath. Disposition of SC and mesaxonal clefts and changes in intercellular membrane/membrane spacing with increasing hypertonicity of bathing medium has been described by Adelman, Moses and Rice (J. Neurocytol. 6:621-646, 1977). Our ferritin experiments were designed to determine accessibility of the mesaxonal space to various sizes of molecules. Freshly dissected axons were tied off and partially cleaned prior to immersion in ∿ 1% (W/V) ferritin in filtered seawater (FSW) at ∿ 14°C. Little or no penetration of the sheath was seen in untreated controls. After exposure to crystallized trypsin (1 mg/ml) in FSW, rapid and massive penetration of ferritin proteins into the sheath, but not the axon was clearly seen. Preparations then were fixed in appropriate glutaraldehyde medium, post-fixed with OsO_4, dehydrated with ethanol, embedded in Epon 12, and unstained sections (0.1-0.2 μm) examined in the EM. Large numbers of ferritin particles were found throughout the outer sheath zones and especially in BL of trypsin-treated specimens, easily identified by the appearance of an Fe peak in EDAX. None of the ∿ 11 nm ferritin molecules appeared to penetrate into adjacent mesaxonal spaces between SC or the periaxonal space, a result in agreement with the measured width (∿ 10 nm at 1 osmolar) of this space derived from electron micrographs by Adelman et al. (loc. cit.).

W-AM-C11 THE ROLE OF THE CELLULAR MEMBRANE DURING FATIGUE IN THE SARTORIUS MUSCLE OF FROG, *Rana pipiens*. J.M. Renaud, Department of Physiology, University of Ottawa, Ottawa K1H 8M5 "Introduced by Dr. J. Hinke"

When frog sartorius muscles were stimulated at a rate of one contraction per second for three minutes, tetanic tension decreased by about 70-80%. Although pH had a small effect on the rate of fatigue, the recovery of tetanic tension was much faster at pH 8.0 than at pH 6.4. The half-recovery time was about 20 min at pH 8.0, but it was more than one hour at pH 6.4. In the presence of curare which inhibits the neuromuscular junctions, the stimulus strength-tetanic tension relationship was shifted to higher voltage following fatigue at pH 6.4, but not at pH 8.0. This shift suggests that fatigue has an effect on the sarcolemma, especially at low pH. Measurements of resting potential, input resistance and time constant of the cellular membrane further confirm this fatigue effect. Resting potential decreased by about 13-15 mV (-15%) during fatigue at both pH levels. During the recovery period at pH 8.0, resting potential returned to pre-fatigue level in about 20 min, whereas after one hour of recovery at pH 6.4 resting potential was still 9 mV below normal. Input resistance and time constant, both decreased by about 20-25% during fatigue at pH 8.0 and both returned to pre-fatigue level in a similar time course as resting potential. However, when muscles were tested at pH 6.4, the input resistance and time constant increased during fatigue and continued to increase during the recovery period. Moreover, the increases were voltage dependent, the increase being smaller as the magnitude of the injected current was increased. Such voltage-dependent changes in input resistance and time constant were not observed at pH 8.0. These results suggest that fatigue has an effect on the properties of the cellular membrane and that the cellular membrane might be involved in the process of tension recovery following fatigue.

W-AM-C12 ION CHANNEL ACTIVITY IN ISOLATED MURINE OLFACTORY RECEPTOR NEURONS. R.A. Maue* and V.E. Dionne, Division of Pharmacology, University of California, San Diego, La Jolla, California 92093

In the presence of odorants, olfactory receptor neurons change their electrical activity. However, the mechanism underlying this response is unknown. To understand the physiology of these neurons, we have begun to characterize their membrane ion channels and define the role of these in the odorant response. We are studying freshly dissociated olfactory receptor neurons from 3-4 month old heterozygous athymic mice with the patch clamp technique. Neurons are isolated by incubating the olfactory epithelium in trypsin and DNAase solutions followed by gentle trituration. The isolated cells are then plated onto concanavalin A coated glass coverslips to hold them in place and studied in HEPES-buffered saline solutions containing 9.4 mM glucose. When viewed under Nomarski optics the neurons retain their major morphological characteristics, and many exhibit fine cilia attached to the distal knob of their dendritic process. "Inside-out" membrane patches excised from both dendritic knob and soma show several kinds of spontaneously active ion channels. With normal extracellular saline in the pipette and elevated K^+ saline in the bath at room temperature, channels of ∿80 pS and 20 pS are found which exhibit distinctly different kinetic behavior. Although both channels appear to be largely K^+ selective, the permeability of the larger channel to other cations may be substantial, as indicated by the difference between its reversal potential and E_K. Internal Ca^{++} concentration does not appear to alter the activity of either channel type. When both membrane faces are exposed to elevated K^+ salines, the conductance of the larger channel is ∿140 pS. Under these ionic conditions application of TEA (30 mM) or 4AP (10 mM) to the cytoplasmic face does not block either channel type, although Cs^+ (50 mM) may block the larger channel.

W-AM-C13 A.C. ANALYSIS OF THE ELECTRICAL STRUCTURE OF MOUSE SPINAL NEURONS IN CULTURE.
Peter B. Guthrie and Gary L. Westbrook (Intr. by Daniel L. Gilbert) , Lab. Developmental Neurobiology, NICHD, NIH, Bethesda MD 20205.

The complex morphological structure of most neurons results in a complex electrical structure. We have used complex sinusoidal stimuli to analyze the electrical structure of primary cultures of embryonic mouse ventral horn (VH) and dorsal root ganglia (DRG) neurons.

Whole-cell patch voltage recording was performed in medium containing 1uM TTX. Complex stimuli of 50 linearly summed sinusoidal currents (1-500Hz) were presented by computer; current monitor and electrode voltage outputs were averaged for 16 continuous presentations. Magnitudes and phase-shifts were obtained using a discrete fourier transform. Small currents (0.01-0.1nA) and small voltages (1-5mV) reduced activation of nonlinear membrane properties. After physiological analysis, the neuron was filled with Lucifer Yellow for morphological reconstruction.

A.C. properties of several simple neuronal models were compared with the experimental data obtained from neurons. In no case could a neuron be adequately modelled as a simple isopotential sphere. A simple ball-and-stick model could adequately describe less than half of the neurons. Phase-shift curves proved particularly effective in differentiating simple models from the more complex electrical structures represented by the remaining neurons.

Compartmental modelling of the morphologically reconstructed neurons is being used to determine the specific membrane properties necessary to match the experimentally observed electrical behavior. Using this approach, we are also attempting to correlate specific electrical structures with several morphological classes suggested by the Lucifer Yellow fills.

W-AM-D1 MEMBRANE DIFFERENTIATION STUDIED WITH MONOCLONAL ANTIBODIES: UNIQUE CELL SURFACE MOLECULES OF ACTIVATED AND ELICITED MACROPHAGES. Bernard A. Fox and Howard R. Petty, Dept. of Biolgical Sciences, Wayne State University, Detroit, MI 48202.

Cell surface differentiation of macrophages has been examined with the monoclonal antibody technique. Macrophages have been obtained from the peritoneal cavities of C57BL/6 mice following treatment with C. parvum, MVE-2, mineral oil, or thioglycollate. Cell populations were mononuclear phagocytes as determined by a latex bead uptake assay. Macrophages obtained from C. parvum or MVE-2 were activated as judged by enhanced cytostatic activity against two tumor cell lines. Rats were immunized with murine macrophages. Hybridomas were prepared by fusion with a non-secreting myeloma line followed by cloning and subcloning. Clones were selected on the basis of binding to either activiated or elicited macrophages (but not both) using a peroxidase-conjugated second-step antibody. The monoclonal antibodies produced have been characterized by flow cytometry. An antibody designated MAA-1 reacts well with activated macrophages but not elicited cells, erythrocytes, or thymocytes. Another monoclonal antibody designated MEA-1 recognizes a molecule on the surface of elicited, but not activated macrophages. Preliminary fluorescence intensification/video microscopy data will be presented. These studies show that certain cell surface membrane structures appear and disappear depending upon the state of differentiation of the cells involved. [Supported by NIH grant 19075-02 to H.R.P.]

W-AM-D2 MACROPHAGE IMMUNE COMPLEX RECEPTORS: STUDIES WITH A NEW FLUORESCENCE - AND LACTOPEROXIDASE-CONJUGATED FERRITIN-ANTI-FERRITIN COMPLEX. William Dereski and Howard R. Petty, Department of Biological Sciences, Wayne State University, Detroit, MI 48202.

A fluorescein- and lactoperoxidase-conjugated ferritin-antiferritin immune complex has been prepared for cell surface labeling experiments. Lactoperoxidase (LPO) has been covalently coupled to affinity-purified anti-ferritin (FT) antibodies with p-benzoquinone by a modified version of Ternynck and Avrameas' method. The conjugate is a heterodimer with linkages to either or both the heavy and light chains of the antibody as judged by two-dimensional SDS-polyacrglamide gel electrophoresis in the absence and presence of 2-mercaptoethanol. The conjugate retains antibody-binding activity as measured by a quantitative precipitin assay. When incorporated into immune complexes the modified antibody also retains Fc recepter recognition ability as determined by erythrocyte-antibody rosette inhibition assays. Electron microscopy demonstrated that the antigen, FT, was monodisperse with complete apoprotein sheaths surrounding the core. FT-anti-FT-LPO complexes were formed in four-fold antigen excess. Complexes were verified by fluorescence and electron microscopy. Immune complexes were then masked with "cold" iodine by use of the endogenous LPO activity. The complexes bound to cells at 4°C as shown by electron microscopy and fluorescence video/intensification microscopy. The LPO delivered to the cell surface in this fashion can be utilized to iodinate the surface with ^{125}I. Under saturation conditions, the labeling with local LPO delivery followed by SDS-PAGE and auto radiography is identical to labeling with free LPO. This labeling approach is of exceptional flexibility and should have wide applicability. [Supported by a grant from the NIH 19075-01]

W-AM-D3 FLOW CYTOMETRY AND FLUORESCENCE INTENSIFICATION MICROSCOPY OF MACROPHAGE CELL SURFACE LDL AND ACETYL-LDL RECEPTORS. Marcia Berry*, Steven Sapareto+, and Howard R. Petty*, *Dept. of Biological Sciences, Wayne State Univ., Detroit, MI 48202 and +Dept. of Experimental Therapeutics, Division of Medical Oncology, Wayne State Univ., Detroit, MI 48202.

Macrophage recognition and endocytosis of DiI-labeled low density lipoprotein (LDL) and acetyl-LDL was studied using fluorescence flow cytometry (FC) and fluorescent video intensification microscopy. RAW264 macrophages, a murine cell line, and a human monocyte-like line (U937) were grown in the tissue culture media in the presence and absence of LDL. LDL was purified and acetylated as described (Basu PNAS 73:3178). Purity and acetylation were verified by SDS-PAGE and IEF, respectively. Forward light scattering indicated that there were uniform in size and that few dead cells or cell debris was present. Several lines of evidence indicate that receptor (R)-mediated endocytosis is taking place. Binding can be distinguished from binding plus endocytosis by incubation at 4 and 37°C, respectively. Binding is trypsin-sensitive. Unlabeled LDL or AcLDL compete for their respective RS. Binding at 4°C is saturable. Uptake at 37°C is time- and ligand dose-dependent. Macrophages grown in the presence or absence of LDL demonstrated distinct labeling patterns. LDL RS were significantly increased by culturing in defined medium without serum lipoproteins. AcLDL RS were unaffected. FC can provide an important tool to examine R levels, modulation of these levels, and R-mediated endocytosis. VIM of similarly labeled cells has been performed. RS appear as punctate fluorescence usually distributed randomly across the cell surface. These studies provide evidence relevant to cholesterol homeostasis and foam cell formation in arteriosclerosis. [Supported by NSF and Mich. Heart Assoc. grants to H.R.P. and NIH to S.S.]

W-AM-D4 MOBILITY OF LECTIN RECEPTORS ON FROG MUSCLE CELL SURFACE. Richard E. Weiss, Walter Stühmer & Wolfhard Almers, Physiol. & Biophys. Dept., Univ. of Washington, Seattle, WA 98195.

Bundles of 1-3 muscle fibers were dissected from the semitendinosus of Rana temporaria and incubated for 20-45 min with one of two divalent fluorescein-conjugated lectins, wheat germ agglutinin (WGA) and succinyl-ConA (sConA). Both lectins bound tightly to sarcolemma and/or basal lamina since the fiber surface retained a fluorescence that was stable for > 3 hrs after washout of the lectin. Mobility of lectin receptors in the plane of the cell surface was measured with "fluorescence recovery after photobleaching," using a 5-7 μm diameter spot of blue light. Measurements were made at 22°C in Ringer and in a relaxing solution (RS) containing no Ca^{++}, 20 mM EGTA and 96 mM KCl. With sConA, measurable recovery never took place; the upper limit for the diffusion coefficient of sConA receptors is 3×10^{-12} cm^2/s. With WGA, 65% ± 7% (S.E.M., n = 12) of the bound WGA appeared mobile; recovery of fluorescence in RS was well fitted with a diffusion coefficient of 4.7×10^{-11} cm^2/s (± 0.6×10^{-11} cm^2/s S.E.M., n = 12). Recovery time courses in Ringer varied widely. Evidently, sConA only binds to immobile cell surface receptors, such as the basal lamina, while WGA binds also to mobile cell membrane receptors, such as integral membrane glycoproteins. Pre-irradiation of the sarcolemma with ultraviolet light (2-3 J/cm^2 at 289 or 302 nm) had no measurable effect on the mobility of WGA receptors. This argues against the possibility that the previously observed immobility of sodium channels in frog muscle sarcolemma (Stühmer & Almers, PNAS 79, p. 946) is a result of UV irradiation. Supported by grants from the NIH (AM-17803 and AM-06915 to REW) and the Muscular Dystrophy Association.

W-AM-D5 MOLECULAR COUNTING IN SMALL CLUSTERS OF LDL ON CELL SURFACES BY FLUORESCENCE INTENSITY QUANTIZATION. David Gross and Watt W. Webb, School of Applied and Engineering Physics, Clark Hall, Cornell University, Ithaca, New York 14853.

Single molecules of the fluorescent analog diI-LDL (Barak and Webb, J. Cell Biol. 90:595, 1981) are visible by fluorescence microscopy. We have employed them as counting markers to determine the size of clusters of LDL receptors on two cell types, human fibroblasts and human epithelial carcinoma cells. The fluorescence intensities were obtained by integrating over the area of observed fluorescent spots in the digitized video image of a cell. The spatial variation of the illuminating light as well as that of the camera response were compensated by computer image processing. Measurements of the probability distribution of intensities of single diI-LDL molecules plated on a glass slide were consistent with Poisson statistics with a mean number of about 40 independent fluorescent groups per diI-LDL. Computer fits to the intensities on cells gave the cluster size (n-mer) distribution. The locations of the n-mers were displayed through the digital video system. We find that the internalization-deficient J.D. mutant fibroblasts GM2408A (Anderson, Goldstein and Brown, Nature 270:695, 1977) and the flat borders of A-431 carcinomas (Anderson, Brown and Goldstein, J. Cell Biol. 88:441, 1981) have more monomer than dimer liganded LDL receptors with no higher n-mers detected on their surface membrane, while normal fibroblasts, GM3348, have equal numbers of monomers and dimers, with larger numbers of higher n-mers. These results support the EM evidence of malfunctioning receptor binding to coated pits on J.D. cells.

Supported by NSF grant 83-03404.

W-AM-D6 TRAPPING OF RECEPTORS BY COATED PITS: THE EFFECT OF TWO DIMENSIONAL DIFFUSION, Jose Ramirez and Joel Keizer, Chemistry Department and Graduate Group in Biophysics, University of California, Davis, CA 95616.

Using the mechanistic statistical theory of nonequilibrium thermodynamics, we have calculated the steady state radial distribution function for LDL receptors around clathrin coated pits. The calculation includes the elementary processes of binding of receptors to pits, diffusion of receptors, and invagination of the pits. The radial distribution function can be written in terms of a McDonald function of order zero and depends explicitly on the trapping rate constant (k^+), the invagination lifetime ($1/\lambda$), the two dimensional diffusion constant of receptors (D_r), and the rate constant for release of receptors from a pit (k^-). We use the radial distribution function to obtain a self-consistent expression for the trapping rate constant, k^+. Using experimental data for LDL receptors, we obtain values for k^+ and k^- which allow us to determine the magnitude of the effect of diffusion on the trapping process.

W-AM-D7 THE AGGREGATION OF DIVALENT CELL SURFACE IMMUNOGLOBULINS BY RIGID POLYVALENT ANTIGENS: MODEL AND EXPERIMENT. B.G. Barisas (Intr. by T.N. Solie), Departments of Chemistry and Microbiology, Colorado State University, Fort Collins, CO 80523

A new model permits calculation of sizes and structures of cell surface aggregates formed at equilibrium between bivalent surface immunoglobulin (sIg) and a rigid polyvalent antigen (Ag) like DNP-polymerized flagellin. The sIg and Ag are assumed to be present at fixed total amount on the cell surface and at constant solution concn., respectively. By assuming a trial free sIg concn., the concns. of aggregates involving i-sIg and k-Ag molecules are evaluated. New methods permit summing in closed form the concns. of all such aggregates to k=∞. Using this sum, the free sIg concn. is evaluated iteratively from the total sIg concn. The distribution of sIg and Ag among aggregates of various structures is then known explicitly. Realistic values of thermodynamic parameters predict that, in situations relevant to immunology, 2-D gelation can occur. This is the appearance of large aggregates (gel) in equilibrium with appreciable amounts of finite-sized aggregates. Calculations suggest 1) Finite aggregates involve $\tilde{<}2$ Ag molecules. 2) <i> per finite aggregate increases with Ag concn. below the gel point. 3) Above the gel point finite aggregate size remains approximately constant and bound Ag enters the gel phase. 4) The fraction of bound Ag in the gel phase under otherwise constant conditions depends strongly on initial sIg density. These predictions are tested against our published photobleaching data on the mobility of Ag-sIg complexes on cells and liposomes and against new cell sorter data on binding of polyvalent Ags to liposomes bearing Ag-specific sIg. Results relate to the physicochemical nature of immunogenic and tolerogenic signals on lymphocytes. Supported by grants NSF PCM 81-11385 and NIH AI 00506.

W-AM-D8 SIGNAL TRANSDUCTION AND LIGAND-RECEPTOR DYNAMICS IN THE NEUTROPHIL. L.A. Sklar and P.A. Hyslop. Dept. of Immunology, Scripps Clinic and Research Foundation., La Jolla, CA 92037

Neutrophils generate free radicals of oxygen, release proteases, chemotax, and phagocytose particles in response to specific ligand-receptor interactions. Evidence suggests roles for Ca^{++} and cAMP in signal transduction. In order to understand the molecular basis of cell activation, we are defining the quantitative relationship between the occupancy of neutrophil N-formyl peptide receptors and cell responses. Quin 2 has been used to examine intracellular Ca^{++} levels in cell response. Since the Ca^{++} levels rise even if EGTA is added to the medium just prior to stimulation, it appears that Ca^{++} is released from an intracellular pool. While the resting level of free Ca^{++} (150 nM) is sensitive to external Ca^{++}, no stimulated Ca^{++} influx is detected during the initiation of cell activation. When intracellular Quin 2 is varied from 0.5 to 5 mM, cellular production of free radicals is effectively inhibited. However, the increment in Quin 2 fluorescence is constant and saturates at a level corresponding to 200 uM Ca^{++} available for Quin 2 binding. This quantity appears to reflect the total store of Ca^{++} released by this receptor. The transient Ca^{++} elevation is saturated with 5 percent occupancy, but nearly all the receptors contribute to the time course of the response. If ligand binding is interrupted, the Ca^{++} level decays with a half time of 10 seconds. We have tentatively divided responses into classes: those whose magnitude parallels the Ca^{++} elevation and require no more than 10 percent occupancy and those whose time course parallels the time course of Ca^{++} elevation. The first includes cAMP elevation, degranulation, shape change, membrane potential dyes responses, and the rate of O_2^- production. The second includes the time courses of O_2^- and cell aggregation both of which decay parallel to Ca^{++} when binding is interrupted.

W-AM-D9 DETERMINATION OF RECEPTOR BINDING CONSTANT IN THE PRESENCE OF COUPLED REACTIONS. J.S. Beck, D. Boland and H.J. Goren, Faculty of Medicine, University of Calgary, Canada, T2N 4N1.

Binding of ligand to receptor is often coupled with other reactions in which free ligand, free receptor or ligand-receptor complex participate. Such reactions often make the usual representations of binding data - such as those where ligand, receptor or complex is degraded - difficult to interpret. In some cases, it is impossible to determine reaction parameters from equilibrium studies. Such cases do, however, produce maxima in the ligand-receptor association curves. By using values of free ligand, free receptor and complex concentrations at times of such maxima, a reaction parameter K_D' can be computed. In the cases of free ligand degradation and free receptor loss, $K_D' = K_D$, the equilibrium dissociation constant. In the case of complex loss $K_D' = K_D + k_c/k_a$, where k_c is the rate constant for the loss of complex and k_a is the ligand-receptor association rate constant.

To simulate association experiments, we have used a fourth-order Runge-Kutta procedure programmed for the HP85A microcomputer (Hewlett-Packard) to solve the sets of differential equations representing the coupled binding and side reactions. Scatchard analysis of simulated association data shows that use of the maxima yields linear plots whereas use of concentrations at an arbitrary fixed time yields curvilinear plots.

With data obtained from a system in which ligand degradation occurs we have produced by this association-maxima method a linear Scatchard-type plot and an estimate of K_D unavailable by conventional methods.

Supported by the Medical Research Council of Canada

W-AM-D10 ANTIBODIES AGAINST TRANSDUCIN CROSS-REACT WITH THE INHIBITORY GTP-BINDING PROTEIN OF THE ADENYLATE CYCLASE SYSTEM IN DIVERSE TISSUES. Samuel E. Navon, Eva J. Neer, and Bernard K.-K. Fung, University of Rochester Medical Center, Rochester, NY 14642 and Brigham and Women's Hospital and Harvard Medical School, Boston, MA 02115.

Transducin, a guanine nucleotide-binding regulatory protein, mediates the signal coupling between rhodopsin and a cylcic GMP phosphodiesterase in vertebrate retinal rods. Affinity-purified antibodies against the T_α and $T_{\beta\gamma}$ subunits of transducin were prepared and used to identify cross-reacting proteins in tissues other than the retina. A 36,000-dalton polypeptide immunologically related to the β polypeptide chain of $T_{\beta\gamma}$ has been found in all tissues tested and is especially abundant in the brain. This polypeptide has been identified as a subunit of the GTP-binding protein (N) of the adenylate cyclase system. Moveover, anti-T_α antibodies also react with a 39,000-dalton polypeptide in isolated brain protein fractions that are highly enriched with inhibitory N protein. This cross-reacting polypeptide can be ADP-ribosylated with Bordetella pertussis islet activating protein but not with cholera toxin. Our results demonstrate that transducin and the inhibitory GTP-binding protein share similar antigenic determinants and are members of a family of signal transducing proteins.

W-AM-D11 THE FAT CELL BETA$_1$-ADRENERGIC RECEPTOR: EVIDENCE FOR ESSENTIAL DISULFIDE BONDS. Cary P. Moxham and Craig C. Malbon. Dept. of Pharmacology, SUNY at Stony Brook, N.Y. 11794

The beta$_1$-adrenergic receptor (BAR) from rat adipocyte membranes has been solubilized and purified in the presence of digitonin by affinity chromatography on a Sepharose-alprenolol matrix and several passes on steric exclusion columns using high pressure liquid chromatography (HPLC). The purified BAR migrates with M_r=67,000 in steric exclusion HPLC. Polyacrylamide gel electrophoresis of radioiodinated purified receptor in 0.1% sodium dodecyl sulfate (SDS) under reducing conditions reveals a single 67,000-M_r peptide. The purified receptor displays pharmacological properties consistent with those of the BAR in the native membrane. When purified radiolabeled BAR was subjected to electrophoresis on polyacrylamide gels in SDS under native, non-reducing conditions, it migrated with greater mobility, M_r=57,000. Treating the native form of the receptor with beta-mercaptoethanol (0.03-10%) or dithiothreitol (0.03-10 mM) decreased the electrophoretic mobility of the native receptor and generated several discrete forms of the BAR, M_r=57,000 to 67,000. Treating purified BAR with 50 μM [^{3}H]-N-ethylmaleimide (NEM) does not result in incorporation of radiolabel into the purified receptor. Treating purified adipocyte membranes with 1 mM NEM, followed by incubation with isoproterenol and 50 μM [^{3}H]-NEM resulted in the incorporation of radiolabel into a membrane protein M_r=70,000. In preliminary studies the amount of (-)[^{3}H]-dihydroalprenolol binding in adipocyte membranes is found to decrease following incubation of the membranes with isoproterenol and NEM in combination, but not with NEM alone. The role of disulfides in the activation of BAR by beta-adrenergic agonists is under intense investigation. (Supported by USPHS grants AM25410 and AM30111).

W-AM-D12 SUBCELLULAR FRACTIONATION OF LIVE CELLS: THE OLIGODENDROCYTE PLASMA MEMBRANE S. Szuchet, P.E. Polak* and S.H. Yim*. Univ.Chicago,Dept.Neurol,5841 S. Maryland,Chicago,IL 60637.

Oligodendrocytes (OLG) generate CNS myelin by enwrapping axons with extensions of their plasma membrane (PM). Myelin has been well characterized but little is known on OLG PM. We have developed a procedure using isolated and live OLG that yields a highly purified PM fraction. OLG were isolated from ovine brains as described (Szuchet et al.J.Neurosci.Meth.3:7-19,1980) and kept in vitro for 4 days. After harvesting, cells were washed, resuspended in 20mM Tris,0.12M NaCl,1mM $MnCl_2$,pH 7.4 (D-medium), broken with a cell disrupter (Szuchet & Polak,Anal.Bioch.128:453-458, 1983), collected in D-medium+1mM EDTA and spun at 300g for 7 min. The pellet contained mostly nuclei. The supernatant was applied on a gradient of 20% percoll in D-medium+EDTA and centrifuged at 30,000g for 15 min. Three bands separated: F1,F2, & F3 (T to B). F2 was PM enriched; F1 & F3 were microsomal and mitochondrial fractions. F2 was further purified by 3 hypotonic washes with 1mM Tris pH 7.4; the final pellet was resuspended in 1mM Tris+1mM $MgSO_4$, left at 4°C for 30 min, applied on a step gradient made of Ficoll in 1mM Tris + 1mM $MgSO_4$ (δ=1.090) and spun at 485,000g for 150 min. The PM fraction (F2.2) was collected at the interphase. F2.2 was enriched relative to the homogenate: 28 fold in K^+-dependent p-nitrophenylphosphatase; 0.06 fold in NADH-cytochrome C reductase and had no mitochondrial membranes. The protein profile of F2.2 (SDS-PAGE) was distinct from that of the other fractions and from the cells. EM studies indicate that isolated PM has a tendency to form myelin-like structures. F2.2 should prove valuable for characterizing oligodendrocyte PM and its changes over time in culture and for comparative studies with myelin. Supported by grant from the National Multiple Sclerosis Society RG-1223-B3.

W-AM-E1 PROTON TRANSLOCATION BY SYNTHETIC ANALOGS OF BACTERIORHODOPSIN. THE ROLE OF THE POLYENE SIDE CHAIN LENGTH AND POINT CHARGE AT THE RING BINDING SITE. Masami Okabe, Valeria Balogh-Nair, Koji Nakanishi, Department of Chemistry, Columbia University, New York, N.Y. 10027.

Bacteriorhodopsin (bR) analogs 1, 2 and 3 were prepared from synthetic 5,6-, 7,8- and 9,10-dihydroretinals. The pigments had absorption maxima at 475, 448 and 335 nm respectively. 1, 2 and 3 were incorporated into asolectin vesicles, the vesicles were continuously illuminated at wavelengths close to the pigment absorption maxima, and the proton translocation, or alkalinization of the medium, was monitored in unbuffered KCl at 30± 0.1°. Proton translocation by analog 1 was only ca. 30% of that of bR regenerated from trans retinal whereas analogs 2 and 3 did not translocate protons. Hence the full conjugated system is necessary for efficient proton pumping.

We had proposed the external point charge model for bR in which, in addition to the counterion of the protonated Schiff base linkage, a charged group close to the β-ionone ring interacts with the conjugated system. This interaction is severely hampered in the 5,6-dihydro analog and almost absent in the 7,8- and 9,10-dihydro analogs. Comparison of proton pumping abilities suggests that interaction between the charged group and the conjugated system may be essential for proton translocation.

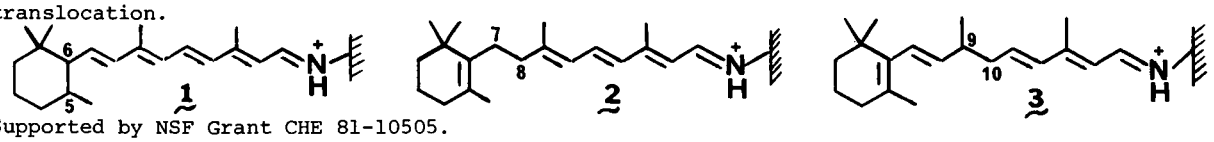

Supported by NSF Grant CHE 81-10505.

W-AM-E2 DARK-ADAPTED BACTERIORHODOPSIN CONTAINS 13-CIS,15-SYN AND ALL-TRANS,15-ANTI RETINAL SCHIFF-BASES. G.S. Harbison and J. Herzfeld, Biophysical Laboratory, Harvard Medical School, Boston, MA 02115; S.O. Smith and R. Mathies, Department of Chemistry, University of California, Berkeley, CA 94720; P.P.J. Mulder, H. Pardoen and J. Lugtenburg, Department of Chemistry, University of Leyden, Leyden, The Netherlands; R.G. Griffin, Francis Bitter National Magnet Laboratory, Massachusetts Institute of Technology, Cambridge, MA 02139.

We have obtained ^{13}C NMR spectra using magic-angle sample spinning for nine ^{13}C-retinyl-labelled derivatives of bacteriorhodopsin. The seven labelled olefinic positions all show a pair of lines due to the coexisting 13-cis and all-trans isomers in dark adapted bR. Except for ^{13}C-14, the chemical shifts observed are close to those of protonated retinal Schiff-bases in solution. The chemical shift of the 13-cis ^{13}C-14 labelled bR is 110.5 ppm, 8 ppm upfield of the solution value for protonated 13-cis retinal Schiff bases. The chemical shift tensor has also been obtained and shows a large upfield shift in σ_{11}. We conclude that these upfield shifts arise from the so-called γ effect caused by steric interaction across a cis double bond between protons 3 carbons distant from each other. Hence we infer that the 13-cis isomer in dark-adapted bR is 15-syn, while the all-trans isomer, with a relatively normal shift of 122.0 ppm for the C-14 position, is 15-anti. We have corroborated this conclusion by demonstrating comparable effects on the isotropic chemical shifts and the chemical shift tensors in protonated aldimines and ketimines, and in retinal derivatives. In contrast, other possible origins for the upfield shift leave σ_{11} unchanged. Finally, our work suggests that the published chemical shifts for solubilized ^{13}C-14 rhodopsin are consistent only with an anti configuration about the C=N linkage in that visual pigment.

W-AM-E3 DETERMINATION OF RETINAL SCHIFF BASE CONFIGURATION IN BACTERIORHODOPSIN AND ITS PHOTOINTERMEDIATES. S.O. Smith, A.B. Myers, J.A. Pardoen, C. Winkel, P.P.J. Mulder, J. Lugtenburg and R. Mathies. Department of Chemistry, University of California, Berkeley, CA 94720.

Resonance Raman spectra of the BR_{568}, BR_{548}, K_{625} and L_{550} intermediates of bacteriorhodopsin have been obtained in H_2O and D_2O using purple membrane regenerated with 14,15-di[^{13}C] and 12,14-dideuterio derivatives of retinal. These derivatives were selected to determine the contribution of the C_{14}-C_{15} stretch to the normal modes in the 1100-1400 cm^{-1} fingerprint region, and to characterize the coupling of the C_{14}-C_{15} stretch with the NH rock. Normal mode calculations demonstrate that when the retinal Schiff base is in the C=N *cis* configuration, the C_{14}-C_{15} stretch and NH rock are strongly coupled, resulting in a large ($\sim$50 cm^{-1}) upshift of the C_{14}-C_{15} stretch upon deuteration of the Schiff base nitrogen. In the C=N *trans* geometry these normal modes are weakly coupled and only a slight (< 5 cm^{-1}) upshift of the C_{14}-C_{15} stretch is predicted upon N-deuteration. In BR_{568}, the insensitivity of the 1201 cm^{-1} C_{14}-C_{15} stretch to N-deuteration demonstrates that its retinal C=N configuration is *trans*. The C_{14}-C_{15} stretch in BR_{548}, however, shifts up from 1167 cm^{-1} in H_2O to 1208 cm^{-1} in D_2O indicating that BR_{548} contains a C=N *cis* chromophore. Thus, the conversion of BR_{568} to BR_{548} involves isomerization about the C=N bond in addition to isomerization about the C_{13}=C_{14} bond. The insensitivity of the native, 14,15-di[^{13}C] and 12,14-dideuterio K_{625} and L_{550} spectra to N-deuteration argues that these intermediates have a C=N *trans* configuration. Thus, the photochemical conversion of BR_{568} to K_{625} involves isomerization about the C_{13}=C_{14} bond alone.

W-AM-E4 ACYCLIC-RETINAL PIGMENT ANALOGUES OF BACTERIORHODOPSIN. R.K.Crouch, W.S.Ghent, Y.S.Or, T.G.Ebrey, and C.H.Chang. Medical University of South Carolina, Charleston, SC 29425 and University of Illinois, Urbana, Illinois 61801.

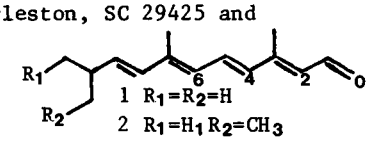

1 $R_1=R_2=H$
2 $R_1=H_1\,R_2=CH_3$
3 $R_1=R_2=CH_3$

The acyclic retinals 1-3 have been synthesized and the all-trans, 2-cis, 6-cis, and 2,6 dicis isomers of each isolated (λ_{max}356-365nm). On combination of each of these retinals with bacterioopsin in the dark an increase in absorption at 450-490nm is observed. The pigments from the all-trans and 2-cis isomers of 1-3 show a single absorption maximum, are stable to the addition of all-trans retinal or hydroxylamine, and form at the same rate as regenerated bacteriorhodopsin. On irradiation of the pigments at 4°C, light adapted forms are obtained. M intermediates and light induced pH changes are observed. Thus, bacteriorhodopsin does not appear to have a specific ring or ring-methyl requirement for binding (in contrast to rhodopsin) and the cyclohexyl ring is not required for photochemistry or proton pumping.

The 6-cis and 2,6 dicis 1-3 pigments do not have a single absorption band. These pigments are mildly unstable to hydroxylamine and all-trans retinal. However, irradiation of these pigments generates single pigments, identical to the corresponding all-trans 1-3 pigments, which do not revert to the mixture on dark adaption. Extraction of chromophores from the light adapted forms showed the retinals to be in the all-trans conformation. These results indicate that a number of cis isomers of retinal analogues having no steric bulk in the ring portion may fit into the binding site of bacterioopsin to form moderately stable dark adapted pigments. Supported by NIH grants EY04939 and EY01323 and NSF grants BNS-80-11563 and PCM-83-40569.

W-AM-E5 FLUORESCENCE ENERGY TRANSFER FROM PARANARIC ACID TO BACTERIORHODOPSIN IN PURPLE MEMBRANE SHEETS, Drake C. Mitchell and G. W. Rayfield, Dept. of Physics, University of Oregon, Eugene, Or 97403. Electron diffraction measurements have led to a determination of the overall three dimensional structure of bacteriorhodopsin. However, electron diffraction cannot, at present, resolve the retinal chromophore of BR. In order to locate the chromophore within the protein structure we have selected a fluorescent probe and the technique of fluorescence energy transfer. The probe we chose is a conjugated polyene fatty acid; paranaric acid (9,11,13,15-octadecatetraenoic acid). Several characteristics make it uniquely suited to our purpose. Its absorption spectrum has the three peak profile typical of conjugated polyenes, with the longest wavelength peak at 314 nm. The emission spectrum consists of a single broad peak with a maximum at 410 nm. These spectral characteristics have allowed us to use paranaric acid in two ways: as an accepter of tryptophan excitation and as a donor of excitation to retinal. Due to its small size and shape we expect that environmental perturbations caused by the insertion of the paranaric acid will be minimal. Insertion was accomplished by incubating a solution of purple membrane sheets and adding microliter aliquots of paranaric acid in ethanol. We believe the paranaric acid inserts itself into the lipid matrix of the purple membrane. Using the Forster formalism and measurements of the efficiency of transfer we calculated the tryp-Pn.A. and Pn.A.-retinal distances. Previous calculation of the tryp-retinal distance makes it possible to use a triangulation technique for fixing the most probable location of the chromophore. Retinal free membranes were obtained both by hydroxylamine bleaching and from a retinal-free mutant of Halobacterium halobium.

W-AM-E6 EFFECTS OF pH AND TEMPERATURE ON CHARGE DISPLACEMENTS IN BACTERIORHODOPSIN
G. W. Rayfield, Physics Dept., University of Oregon, Eugene, Oregon 97403

An analysis of the photoresponse of bacteriorhodopsin yields information on the time course of charge displacements within the protein. This work presents the effect of pH and temperature on these charge displacements. Photoactive membranes were formed by depositing bacteriorhodopsin on a thin (6 micron) teflon sheet separating two aqueous electrolyte solutions. A high power dye laser excites the photoactive membrane and a photoresponse is recorded on a Nicolet 4094 digital oscilloscope. Slow components (τ>20 μsec) of the photoresponse are measured as photo currents while faster components (τ>1μsec) are measured as photovoltages. Data is transferred to an IBM PC microcomputer and analyzed with a non linear least squares fitting program (Marquardt algorithm) for a sum of exponentials. The amplitudes and time constants derived from the fitting program are interpreted in terms of charge displacements within the protein. The effect of temperature and pH on these parameters will be presented. Temperature was varied from -20°C to 30°C and pH from 3 to 10.
(Supported by NIH grant GM 26669.)

W-AM-E7 USE OF FLUORESCENT DYES TO DETECT HALOBACTERIAL RHODOPSINS: CORRELATION OF s-RHODOPSIN WITH PHOTOTAXIS. Barbara E. Ehrlich[a], Cathy R. Schen[a], and John L. Spudich[a,b], [a]Department of Physiology and Biophysics, and [b]Department of Anatomy, Albert Einstein College of Medicine, Bronx, NY 10461

Three retinal-containing pigments have been detected in Halobacterium halobium membranes: bacteriorhodopsin (bR), halorhodopsin (hR), and s-rhodopsin (sR). The first two hyperpolarize the cell membrane by electrogenic transport of H^+ an Cl^- respectively. The third pigment, sR, may be a photosensory receptor since mutants lacking bR and hR retain their retinal-dependent phototaxis responses. We monitored light-induced changes in fluorescence of several voltage-sensitive dyes in cells and membrane vesicles. Red light-induced potential changes generated by bR and hR were similar to signals described previously by Schobert and Lanyi (J. Biol. Chem. 257: 10306 (1982)). Signals generated by hR could be identified using four criteria: wavelength dependence, Cl^- dependence, shunting by valinomycin and K^+, and the absence of these signals in hR-deficient mutants. The absence (detection limit ~0.5 mV) of hyperpolarization signals in $bR^-hR^-sR^+$ vesicles and cells shows sR photochemical reactions are non-electrogenic. Two signals independent of bR and hR were measured: blue light caused a decrease and red light an increase in dye fluorescence. Both signals appear to derive from sR on the basis of their retinal-dependence and action spectra. In a retinal-deficient mutant strain (Flx3R), both sR signals appeared after addition of all-trans retinal. The retinal-generation of phototaxis and of the sR signals show the same retinal concentration dependence, supporting the hypothesis that sR is a sensory receptor for phototaxis. (Supported by NY Heart Association (BEE) and NIH grant GM 27750 (JLS)).

W-AM-E8 DEVELOPMENT OF MEMBRANE POTENTIAL BY BACTERIORHODOPSIN IN H. HALOBIUM CELL ENVELOPE VESICLES. M.K. Mathew[#], S.L. Helgerson[#], D. Bivin[#], P.K. Wolber[#], W. Stoeckenius[#] and E. Heinz[+]. [#]Cardiovascular Research Institute and Department of Biochemistry and Biophysics, UCSF, San Francisco, CA 94143 and [+]Cornell University Medical College, New York, NY 10021.

Bacteriorhodopsin functions as an electrogenic, light-driven proton pump in H. halobium. In closed membrane systems the bR photocycle kinetics are sensitive to the background light intensity and can be correlated with membrane potential. The initial decay rate of the M photointermediates following laser excitation have been related to steady-state membrane potential, allowing the construction of a calibration curve. The laser (λ=592.5nm) was flashed at various time delays following the start of background illumination (λ=592±25nm) and transient absorbance changes at 415nm monitored in cell envelope vesicles. The vesicles were loaded with and suspended in either 3M NaCl or 3M KCl buffered with 50mM HEPES at pH 7.5 and the membrane permeability to H^+ modified by pretreatment with DCCD. In each case the membrane potential rose with a halftime of ~75msec. The steady-state potential achieved depends on the cation present and the H^+ permeability of the membrane, i.e., higher potentials were developed in DCCD-treated vesicles or in NaCl media as compared to KCl media. The results can be modeled using an irreversible thermodynamics formulation (Heinz, in Hydrogen Ion Transport, Elsevier: Amsterdam, 1980) assuming a constant driving reaction affinity for the pump and the presence of a voltage-dependent, electrogenic Na^+/H^+ antiporter which is active when vesicles are suspended in NaCl.

(Supported by NIH Program Project Grant GM-27057 and NIH GM-26554.)